Shrew is a newly evolved Drosophila gene required for generation of the embryonic dorsal-ventral BMP activity gradient

MaryJane Shimell[1], Robert Connacher[2], Sangbin Park[3], Kavita Arora[3*], and Stuart J. Newfeld[4*], Michael B. O'Connor[1*]

[1] Department of Genetics Cell Biology and Development
University of Minnesota
Minneapolis, Mn 55455

[2] Department of Biochemistry, Molecular Biology and Biophysics
University of Minnesota
Minneapolis, MN 55455

[3] Department of Development and Cell Biology
University of California
Irvine, CA 92697

[4] School of Life Sciences
Arizonia State University
Tempe, AZ 85287

*Correspondence: Michael O'Connor: moconnor@umn.edu
Stuart Newfeld: newfeld@asu.edu

Keywords: dpp, short gastrulation, twisted gastrulation, tolloid, natural selection

Running head: Srw evolution and function

Abstract

Patterning the dorsal surface of the Drosophila blastoderm embryo requires the rapid redistribution of a BMP heterodimer (Dpp-Scw) from lateral regions of the embryo to the dorsal midline as cellularization is completed. This redistribution creates a steeply graded BMP signal with a peak activity in the mid-dorsal region and requires four additional secreted gene products: Short gastrulation (Sog), Twisted gastrulation (Tsg), Tolloid (Tld), and Shrew (Srw). While the functions of Sog, Tsg and Tld, and their vertebrate homologs in generating BMP activity gradients have been well described, the role of Drosophila Srw remains an enigma. Here we show that Srw encodes a secreted, N-terminally truncated version of Tsg that stimulates cleavage of Sog by Tld but without forming a stable interaction with any identified component of the patterning machinery. We further demonstrate that the requirement for Srw can be bypassed simply by providing additional Tsg in *srw* mutant embryos prior to cellularization. Our phylogenetic analysis suggests that the evolution of Srw involved two temporally separate duplications of an ancient Tsg to yield three Tsg-like genes in a subset of Diptera. This was followed only in Drosophila by truncation of one Tsg-like product to form Srw. We speculate that the evolution of Srw resulted from a strong selective pressure for adaptations that accelerate Drosophila embryonic development thereby minimizing egg exposure to predation, parasitism, and environmental stress. Taking into consideration both the evolutionary and biochemical data we outline possible mechanistic models for how Srw stimulates Sog cleavage by Tld to hasten BMP gradient formation in rapidly developing Drosophila embryos.

Introduction

Members of the BMP family of secreted growth and differentiation factors modulate a wide range of developmental processes including stem cell self-renewal, organ growth and differentiation, apoptosis, and early axial specification (reviewed in (Katagiri and Watabe, 2016). In Drosophila, assignment of dorsal cell fate during early embryogenesis requires the activity of two BMP family members, Screw (Scw) and Decapentaplegic (Dpp) (reviewed in Akiyama et

al., 2024; O'Connor et al., 2006; Upadhyay et al., 2017). These factors form both homo and heterodimers and signal through the type II receptor Punt and different complexes of the Type I receptors Thickveins (Tkv) and Saxophone (Sax) to specify early cell fate. Activation of the type I receptors by Punt in response to ligand binding stimulates phosphorylation and nuclear accumulation of phosphorylated Mothers against Dpp (pMad), the only Drosophila BMP specific R-Smad, in a complex with the Co-Smad Medea. The pMad-Medea complex regulates transcription of numerous target genes in the dorsal half of the embryo to assign two primary cell fates within this region. (Ashe et al., 2000; Raftery and Sutherland, 2003; Sutherland et al., 2003). The amnioserosa is derived from approximately 200 cells that straddle the dorsal midline, in response to high levels of BMP signaling. In contrast, lower levels of BMP signaling in flanking dorsal-lateral cells specify the dorsal ectoderm. Overall, dorsal cell fate in Drosophila is governed by BMP ligands acting as classical morphogens to specify these unique fates in a concentration dependent manner (Ferguson and Anderson, 1992a; Wharton et al., 1993).

An unusual feature of this embryonic BMP patterning mechanism is that its output exhibits spatial bi-stability (Wang and Ferguson, 2005). In this case, spatial bi-stability means that there is a sharp transition zone in signal reception between the future amnioserosa and the dorsal ectoderm (i.e., signaling is step-like). This step-like output results from a complex series of interactions between the two BMP ligands and several additional extracellular components (reviewed in (Umulis et al., 2009). These components included a zinc metalloprotease Tld, and two BMP binding proteins Sog and Tsg. Sog and Tsg preferentially form complexes with Dpp-Scw heterodimers preventing them from binding to their receptors in dorsal lateral regions (Shimmi et al., 2005b). Tld cleaves Sog (Marques et al., 1997) releasing the heterodimer from the complex allowing it to either rebind to another Sog-Tsg complex or to receptors. This reiterative cycle of binding and cleavage leads to a net flux of heterodimers to the dorsal midline where the cleavage reaction dominates, and net ligand release occurs (Marques et al., 1997; Mizutani et al., 2005; Shimmi et al., 2005b). The ligand heterodimer then binds to a receptor complex containing Punt and a heterodimer of Tkv and Sax, that in turn stimulates a high level

of Mad phosphorylation and specification of amnioserosa. Dpp homodimers and Scw homodimers have a lower affinity for Sog-Tsg (Shimmi et al., 2005b). Consequently, they are not transported effectively to the midline and remain broadly distributed throughout the dorsal domain where they likely bind to Tkv and/or Sax homomeric complexes that are less effective in signaling compared to the Dpp-Scw heterodimers. In addition to the ligand transport process mediated by Sog, Tsg and Tld, the step-like boundary between high and low pMad signaling is further enhanced by a positive feedback mechanism that involves BMP activation of *eiger*. Eiger then that acts via an incompletely characterized pathway to augment heterodimer binding to receptors in the dorsal-most cells (Gavin-Smyth et al., 2013). In addition, extracellular matrix components such as type IV collagen and integrin also play a role in the shuttling mechanism. These proteins provide an assembly and release platform for incorporating Sog, Tsg, Tld and the BMP heterodimer into various complexes through a series of distinct interactive steps (Sawala et al., 2015; Sawala et al., 2012; Umulis et al., 2009; Wang et al., 2008; Winstanley et al., 2015).

A similar mechanism employing BMP heterodimer transport, complex cleavage and positive feedback has been shown to pattern a subset of Drosophila wing veins during pupal development. Specification of the posterior cross vein (PCV) requires the BMP ligands Dpp and Glass bottom boat (Gbb; reviewed in O'Connor et al., 2006). Once again Dpp-Gbb heterodimers appear to be preferentially bound by Sog and a Tsg paralog called Crossveinless (Cv) whereupon Sog is targeted for cleavage by the Tld paralog Tolloid-related (Serpe et al., 2005; Shimmi et al., 2005a). These interactions produce a net flux of heterodimers away from the longitudinal veins into the presumptive posterior cross vein region and subsequent refinement of the BMP spatial signal through positive feedback. Low level BMP signals induce Crossveinless 2 (Cv-2) that acts as a cell surface localized BMP binding protein that augments BMP signaling likely by facilitating transfer of BMPs to the signaling receptors (Serpe et al., 2008). An additional secreted factor, Crossveinless-d, a patterning in the wing patterning, although its mechanism of action has not been determined (Chen et al., 2012).

Homologs of these Drosophila patterning proteins are found in numerous other invertebrates and vertebrates where they also generate BMP activity gradients. However, in vertebrates, the mechanistic roles played by the various BMP interacting proteins can be quite different (reviewed in De Robertis and Tejeda-Muñoz, 2022) In the Drosophila example interactions of the BMP heterodimer with Sog, Tsg and Tld leads to a redistribution of the heterodimer over time and is referred to as a "shuttling" model. In contrast, in zebrafish a "source-sink" model best fits the available data, while in Xenopus a "counter gradient" model is envisioned (reviewed in Madamanchi et al., 2021). Each of these mechanisms arise as the result of different spatial expression patterns of the various interacting components as well as the individual biochemical reaction parameters (binding affinities, cleavage rates, diffusion characteristics) of the components.

Although a great deal is known about the molecular mechanisms contributing to formation of a BMP gradient in the early Drosophila embryo, the role of Srw (Bonds et al. 2007) continues to be ill-defined. Mutations in *srw* were originally identified in loss-of-function screens for genes that affect embryonic patterning (Jürgens et al., 1984). Subsequently, *srw* was shown to act in the dorsal patterning process and presumed to augment Dpp signaling since its phenotype could be suppressed by additional copies of Dpp (Ferguson and Anderson, 1992b). Previous studies showed that *srw* codes for a molecule related to the C-terminal domain of Tsg family proteins (Bonds et al., 2007). Tsg-like proteins contain a N-terminal BMP binding module (Oelgeschläger et al., 2000) and a C-terminal domain that is capable of binding to one or more of the four von Willebrand factor (VWF) domains of Sog and its vertebrate homolog Chordin (Malinauskas et al., 2024; Moore et al. 2024). The presence of only a C-terminal domain in Srw suggests that it might bind Sog but not BMPs.

In this study, we show that *srw* is ubiquitously expressed in the early embryo and that loss of *srw* leads to very low uniform levels of BMP signaling throughout the dorsal region of the embryo like *sog* and *tsg* mutants. Epistasis experiments in the embryo using double mutant analysis demonstrates that, *srw* functions upstream of *tld*. Although Srw does not appear to be a

stable component of the Sog-Tsg-BMP complex, biochemical experiments suggest that it facilitates the cleavage of this complex under conditions with low Tsg levels. Consistent with this view, we find that injection of additional *tsg* mRNA or maternal deposition of *tsg* can bypass the requirement for *srw* in embryonic patterning.

We also conducted an extensive phylogenetic analysis to identify the evolutionary context for Srw. We found that Tsg appeared before the Deuterostome-Protostome split. Subsequently, sporadic duplications in a subset of Arthropods produced a second Tsg-like protein. In an unidentified species of the Dipteran lineage with a Tsg duplication, diversification led one copy to become Cv. Then in a subset of Diptera a duplication of the Cv-like protein led to species with three Tsg family members. Exclusively in Drosophila, one of the Cv-like proteins was truncated to create Srw with only a C-terminal Sog-binding domain. We discuss the implications of our evolutionary and biochemical findings with respect to the responsible selective pressure and potential molecular mechanisms of Srw function.

Results

The *srw* gene was identified in the embryonic lethal screens by Nusslein-Volhard Wieschaus and Jurgens (Jürgens et al., 1984). Based on the loss of specific cuticular structures, Srw was assigned a role in patterning the dorsal region of the early embryo (Ferguson and Anderson, 1992b). Cloning and molecular characterization of *srw* revealed that it encodes an N-terminally truncated relative of Tsg-Cv (Bonds et al. 2007). To further understand how Srw functions in early embryonic patterning, we isolated a genomic fragment containing the entire *srw* coding region and approximately 3 kb of upstream sequences. This fragment, and a modified construct containing a C-terminal His-tag, were used to generate transgenic lines for additional studies. Transgenic lines on the 2nd chromosome were paired with two different *srw* homozygous lethal mutants (srw^{B4}, srw^{B18}). The paired lines were then crossed to additional *srw* mutants to look for transheterozygous mutant rescued flies. We recovered Mendelian ratios of non-balanced adults using both the tagged and untagged versions of Srw indicating that this

genomic fragment contained all the essential regulatory elements, and that the C-terminal tag does not interfere with Srw function, a critical consideration for tests of biochemical activity.

In the initial cloning study *srw* expression could not be detected by *in situ* hybridization but was inferred to be expressed at low level during early development since it could be PCR amplified from RNA prepared from 0-6 hour old embryos (Bonds et al., 2007). To determine if *srw* expression was spatially restricted in the early embryo, we carried out *in situ* hybridization. We detected specific expression of *srw* in a uniform pattern in the cellular blastoderm and early gastrulation stage embryos (Fig. 1 A, B), which then fades during gastrulation (Fig. 1 C). We could not detect *srw* expression above noise in any other embryonic tissue after germband extension or in third instar larval imaginal discs and the central nervous system.

The early uniform expression of *srw* is unusual since all other genes that specify embryonic dorsal tissues, except *scw* (Arora et al. 1994), show localized expression along the dorsal-ventral (D/V) axis. Both *dpp*, and *tld* are transcribed in the dorsal half of the embryo (Fig 1 D, E, see also Shimell et al., 1991; St Johnston and Gelbart, 1987) while *tsg* expression is restricted to a central dorsal domain (Mason et al., 1994). In contrast, *sog* is expressed in two ventral lateral domains in the blastoderm embryo (Fig 3 F also Francois et al., 1994). Although *scw* is ubiquitously expressed at the blastoderm stage like *srw*, it is presumed that the active Dpp-Scw heterodimer only forms in dorsal domain cells that co-express Dpp and Scw (Shimmi et al., 2005b). The expression of *srw* is also unusual in that it is not observed in imaginal discs. This suggests that Srw is likely only required at the cellular blastoderm stage and may only facilitate shuttling of the Dpp-Scw heterodimer during embryonic development.

The presence of a putative signal peptide at the Srw amino terminus suggests that it is a secreted protein (Fig. S1). To test this, we generated several constructs for expression of C-terminally tagged Srw in Drosophila S2 cells and found that the protein was secreted into the supernatant (Fig. S1), consistent with our expectation. To further aid in structural studies, we sequenced 12 available mutant alleles. The nucleotide and amnio acid changes associated with these alleles are shown in Table 1.

Table 1 Molecular characterization of twelve *srw* alleles.

mutation	base change	amino acid change
srw^{1}	T->A	Cys123->Ser123
srw^{B3}	G->A	Gly94->Arg94
srw^{B4}	G->T	Gly67->stop
srw^{B18}	C->T	Gln23->stop
srw^{10K}	T->A	Cys123->Ser123
$srw^{h2.19}$	G->A	Cys123->Tyr123
$srw^{15.33}$	G->A	Trp55->stop
$srw^{110.18}$	G->A	Gly110->Arg110
$srw^{65.46}$	G->A	Trp55->stop
$srw^{75.41}$	G->A	Trp55->stop
$srw^{34.67}$	G->A	Glu31->Lys31
$srw^{104.20}$	G->A	Met1->Ile1

Next, we used AlphaFold to model the consequences of these mutations on the predicted three-dimensional structure of Srw (Fig. 2). A comparison of the predicted structures of Tsg, Cv, and Srw (Fig. 2 A), shows that putative SOG binding and BMP-binding domains form globular structures separated by short unstructured regions. Additionally, while Srw lacks the N-terminal BMP-binding domain, but the putative Sog binding domain of Srw shows similar folding to Tsg and Cv (Fig. 2 B). The locations of *srw* missense mutants characterized in this study are found throughout the protein (Fig. 2 C). Residues mutated in srw^{B3} (G94R) and $srw^{110.18}$ (G110R) are buried within the presumed SOG binding domain However, $srw^{35.67}$ (E31K) is predicted to be solvent exposed. The cysteines of $srw^{h2.19}$ (C123Y) and srw^{1} (C123S) are predicted to form one of two disulfide bonds that holds the C-terminal tail close to the SOG binding domain (Fig. 2 D). An equivalent disulfide bond is predicted in Cv and Tsg and verified in the human Twisted gastrulation protein homolog1 (TWSG1) crystal structure (Malinauskas et al., 2024). The C123S mutation at this location in srw^{1} implies that this disulfide bond is critical for Srw activity.

Recently, it has been suggested that TWSG1 interacts with the VWF-4 domain of human Chordin and mutations in Drosophila Tsg that disrupt the interaction interface showed altered dorsal embryonic pattering (Moore et al., 2024). Both Tsg and Srw are predicted to interact similarly with the equivalent region of Sog (Fig. 2 E). Specifically, Srw α_2 helix (Tsg α_4) is directly opposed to a bundle of VWF-4 β-sheets (Fig. 2 F). As G94 and G110 are packed tightly

behind this helix, their mutation to a bulky, hydrophilic residue likely disrupts binding.

Shrew is required for Dpp shuttling and amnioserosa cell fate determination.

To assess the role of Srw in the shuttling process more directly, we examined the expression of several embryonic dorsal tissue markers including *rhomboid* (*rho),* pMad (Gavin-Smyth et al.) and Kruppel (Kr) that marks the amnioserosa. Loss of *srw* leads to a failure to refine the dorsal pattern of both *rho* and pMad, like that seen in *tsg* and *sog* mutant embryos, but less severe than that see in *tld*, *scw* and *dpp* mutants (Fig. 3). Refinement of the *rho* and pMad patterns requires the proper shuttling of the Dpp-Scw heterodimer to the dorsal midline (Marques et al., 1997; Shimmi et al., 2005b), therefore, we infer that Srw is also required for this process. This failure in morphogen shuttling ultimately leads to the loss of amnioserosa fate and improper gastrulation in *srw* mutants, (Fig. 3 G) like the phenotypes of *tsg* and *sog* mutants (Ferguson and Anderson, 1992a; Mason et al., 1994). We also examined the *rho* expression profile of a *srw, tld* double mutant (Fig. 3 F) and observed that these double mutants lacked dorsal expression of *rho,* like *tld* mutants. Therefore, we infer that Tld function is epistatic to Srw. In contrast, the *tsg, tld* double mutant has the opposite epistatic relationship where the pattern of the double mutant is like *tsg* (that retains broad expression of *rho*) and not *tld mutants* (Shimmi and O'Connor, 2003).

Srw enhances Tld mediated cleavage of Sog-Dpp or Sog-Tsg-Dpp complexes

We have previously demonstrated that Tsg forms a tripartite complex with Sog and either Dpp homodimers or Dpp-Scw heterodimers (Shimmi et al., 2005b). A similar complex is formed by the vertebrate counterparts, although the exact stoichiometry of Tsg (1 or 2 per complex) in either the Drosophila or vertebrate assemblies is unclear (Oelgeschläger et al., 2000). Since the phenotype caused by loss of Srw, is like that of *sog* and *tsg* loss (Fig. 3), whose products form a stable complex with the Dpp-Scw heterodimer to modulate BMP signaling in the early embryo, we first sought to determine if Srw also formed a stable complex with any of these components. Using S2 cell supernatant expressing a tagged form of Srw, we performed co-immunoprecipitation (Co-IP) experiments using Dpp, Dpp-Scw, Sog, Tsg and Tld with unique combinations of tags on each protein. In no case did we observe Co-IP of Srw with any of these

proteins individually or in different combinations. Thus, we conclude that Srw function utilizes either a transient low affinity interaction with one or more of these molecules or requires an unknown intermediary component.

We next tested whether the addition of Srw could enhance the cleavage of Sog in various combinations of other D/V patterning components. Previous studies showed that the speed of Sog cleavage by Tld in the presence of Dpp or a Dpp-Scw heterodimers is increased by increasing the Tsg concentration (Shimmi and O'Connor, 2003; Shimmi et al., 2005b). We reasoned that the similarity of Srw to the Tsg C-terminal domain may also enhance Tld mediated Sog cleavage. We first identified relative concentrations of Dpp, Sog and Tld that led to slow cleavage of Sog at sites 1 and 2 with no cleavage at site 3 even after 24 hours of incubation (Fig. 4 A, B). Addition of Tsg to the reaction, cause somewhat faster but not sustained cleavage of Sog at sites 1 and 2, and again no cleavage at site 3 (Fig. 4 C). Substitution of Srw for Tsg produced sustained cleavage of Sog at all three sites (Fig. 4 D). Addition of Srw and Tsg together, resulted in even faster and sustained cleavage (Fig. 4 E). Lastly, reducing Tld concentration by half and maintaining equivalent amounts of Srw, Tsg and Sog (Fig. 4 F) cleavage remained equally robust and sustained. These results indicate that Srw enhances Tld proteolytic activity perhaps by inducing a transient conformation of the Sog-Dpp-Tld complex that renders Sog cleavage sites more accessible to Tld.

Srw function is dispensable for viability in the presence of excess Tsg.

Since the primary function of Srw appears to be enhancing Sog cleavage, also an activity of Tsg, (Larraín et al., 2001; Shimmi and O'Connor, 2003), we hypothesized that Srw might be bypassed by providing additional Tsg. We used two different approaches to address this conjecture. First, we injected mRNA of either *tsg* or *srw* into *srw* or *tsg* mutant embryos and scored for rescue by quantifying the number of Kr positive amnioserosa cells formed. Injection of *srw* mRNA into *srw* mutant embryos rescued amnioserosa cell fate in a concentration-dependent manner (Fig. 5). Intriguingly, *tsg* mRNA injections could also rescue *srw* mutants. In a few cases, adults eclosed with no visible morphological defects reinforcing the impression

from *srw* in situ hybridization that there is no additional requirement for *srw* after early embryogenesis. Importantly, injection of *srw* mRNA into *tsg* mutant embryos could not rescue *tsg* mutants which might be expected since Srw does not possess a BMP binding domain. We also tested a chimeric Tsg-Srw molecule that retained the N-terminal BMP binding domain of Tsg but the C-terminal "half" was replaced by Srw sequences. A second chimera contained the same Tsg N- terminal domain followed by Srw sequences that lack the signal peptide and the N-terminal linker region which contains the putative Sog VWF interaction site (Tsg-SrwΔ). Interestingly injection of Tsg-Srw mRNAs gave reasonable rescue of *srw* at low dose but none at high. Injection of the same construct into *tsg* mutant embryos gave no rescue. In contrast, injection of Tsg-SrwΔ resulted in no rescue of either *srw* or *tsg* mutants at either dose. Taken together, these data indicate that at high concentrations, wildtype Tsg can bypass the requirement for Srw for proper D/V patterning, while Tsg-Srw chimeric proteins cannot rescue *tsg* mutants but, depending on the nature of the hybrid protein, can provide some rescue of *srw* mutants.

In a second test, we examined whether simply supplying *srw* or *tsg* maternally would be sufficient not only for embryogenesis but also to produce fully developed fertile adults. We placed *srw* and *tsg* coding sequences in a UASP vector enabling high level maternal expression using suitable maternal promoters driving Gal4 or derivatives (Rørth, 1998). With *mtub.GAL4-VP16* driving either *tsg* or *srw* into *srw* mutant eggs, to maternally load *srw* mutant eggs with either *tsg* or *srw*, we saw complete rescue of *srw* mutants. These crosses yielded Mendelian ratios of adult flies that where viable and fertile with no obvious morphological defects including normal crossveins (Fig. S2). We conclude that Srw is only required during early embryonic development and that this requirement can be bypassed if sufficient Tsg is present.

Paralog analysis in D. melanogaster demonstrates that Srw is most like Cv not Tsg

To provide additional clues to Srw function and shed light on its evolutionary origin, we analyzed the three Tsg family members (Tsg, Cv, and Srw; Fig. S3). First, we generated a full-length alignment of the three Tsg family members and found that Shrew is 66% identical to both Tsg and Cv in a carboxy-terminal 57 amino acid region that contains ten cysteines. Second, a

tree generated from the alignment shows clustering of Srw and Cv, with Tsg more distant. This immediately suggested a birth order of Tsg, Cv then Srw with Srw subsequently losing its BMP binding domain. Third, to further evaluate our hypothesis that Srw serves as an accessory to Tsg that enhances Sog cleavage, we conducted a large-scale phylogenetic analysis employing the highly conserved region. The goal was to identify Tsg proteins in a diverse set of fully sequenced multicellular animals to test this birth order hypothesis.

Origin of Tsg family members identifies Srw as a new Drosophila specific gene

Our study began at the base of the metazoan lineage (multicellular animals) with an examination of two radially symmetric organisms. Their divergence from *Drosophila melanogaster* was over 715 million years ago (mya) and they predate the existence of organisms with bilateral symmetry (Table 2). Exemplar species of the Ctenophora (comb jellyfish) and Cnidaria (sea anemone) do not contain any Tsg family members. Both species have reference genomes with 12- or 53-fold coverage providing some confidence that the absence of Tsg family members is not an artifact.

In the Bilateria (organisms with bilateral symmetry at least during development), the split between the Deuterostome and Protostome superphyla occurred roughly 710 mya. Deuterostomes, including humans, contain a gut with two openings in which the original gastrulation pore becomes the anus. Protostomes, including Drosophila, contain a gut with two openings in which the original gastrulation pore becomes the mouth. We examined 12 Deuterostomes. Two well-known model organisms (sea urchin and house mouse) are shown, and they both have only Tsg. A tree of the *D. melanogaster* proteins with the sole family member in sea urchin *Strongylocentrotus purpuratus* demonstrates that it is clearly Tsg (Fig. S4).

Within Protostomes we found that all members of the oldest phyla (divergence roughly 680 mya), the Mollusca (e.g., octopus), Nematoda (e.g., roundworm) and Priapulida (e.g., marine worm) also have only Tsg. A tree of the Nematoda species *Pristionchus pacificus* with the three *D. melanogaster* proteins reveals the same branching pattern as the sea urchin tree. Interestingly, the model organism *Caenorhabditis elegans* has a complete genome but no Tsg family members.

This is the only example we found of a Bilaterian organism with no Tsg protein. Clearly, Tsg arose early and for nearly 120 million years was by itself sufficient for D/V patterning in Bilaterian species.

In the youngest Protostome phylum Arthropoda (563 mya), a survey of roughly 300 million years showed sporadic examples of species with two Tsg family members. The oldest example is in the subphylum Chelicerata Class Merostomata (horseshoe crabs). The other examples are in the class Insecta (459 mya), although species with Tsg pairs are not closely related (e.g., Hymenoptera and Nematocera). The Hymenoptera species *Nasonia vitripennis* contains Tsg1-A and Tsg1-like that cluster with each other in a tree with *D. melanogaster* proteins when analyzed together, but that cluster with *D. melanogaster* Tsg when analyzed individually (Fig. S4). The Nematocera are Dipterans (true flies) with sequenced species in many genera such as aphid (Aphis), butterfly (Bicyclis), grasshopper (Schistocerca), silk moth (Bombyx), red flour beetle (Tribolium) and water flea (Daphnia). Each of these have one Tsg. A notable exception with a Tsg duplication is mosquitos (Anopheles).

Two further points about the class Insecta are relevant. First, D/V patterning in most of Insects generates two extra-embryonic tissues at the dorsal midline, the serosa and the amnion, rather than a single amnio-serosa as in D. melanogaster (Wotton, 2014). Second, the milkweed bug *Oncopeltus fasciatus* in the Paraneoptera has one Tsg that suppresses Dpp activity ventrally rather than activating Dpp dorsally (Sachs et al., 2015). Nevertheless, the presence of a second Tsg does not correlate either with a specific mechanism or specific type of dorsal tissue.

In the Dipteran suborder Brachycera (256 mya), all species examined have two or three Tsg family members and one of them is always Cv. Thus, in an unidentified species with two Tsg proteins in the Dipteran lineage leading to Brachycera, diversification led one copy of Tsg to become Cv then a duplication of Cv led to species with three Tsg family members. There are two sister superfamilies that diverged 129 mya. In the Calyptratae, the exemplar species *Musca domestica* (house fly) has three Tsg family members, including Cv and a recent duplication of Cv (Fig. S4). The presence of two Cv proteins was shown by our reciprocal BLASTp and 'align

Table 2. Tsg family evolution: Srw is a new gene found only in the genus Drosophila

MYA[a]	Taxon[b] (D. mel lineage red)	Representative Species (RefSeq Y/N[c])	Tsg status[d]
I. Tsg appears prior to Deuterostome-Protostome split roughly 708 MYA			
758	Kingdom: Metazoa	Multicellular animal	
743	Phylum: Ctenophora	Mnemiopsis leidyi (comb jellyfish; Y)	none
715	Phylum: Cnidaria	Nematostella vectensis (sea anemone; Y)	none
743	Clade: Bilateria	Bilateral symmetry during embryonic development	
635	Phylum: Xenacoelomorpha	Meara stichopi (marine flatworm with no gut; N)	1 is Tsg
708	Clade: Deuterostomia	2 opening gut and blastopore becomes anus	
635	Phylum: Echinodermata	Strongylocentrotus purpuratus (sea urchin;Y).	1 is Tsg
319	Class: Mammalia	Mus musculus (house mouse; Y)	1 is Tsg
708	Clade: Protostomia	2 opening gut and blastopore becomes mouth	
686	Phylum: Mollusca	Octopus bimaculoides (California octopus; Y)	1 is Tsg
692	Phylum: Nematoda	Roundworms	
686	Class: Chromadorea	Caenorhabditis elegans (free living in soil; Y)	none - lost
		Pristionchus pacificus (symbiont of beetles; Y)	1 is Tsg
686	Class: Enoplea	Trichinella pseudospiralis (human parasite; Y)	1 like Tsg
686	Phylum: Priapulida	Priapulus caudatus (marine worm unsegmented; Y)	1 like Tsg
II. Tsg duplicates appear sporadically in Arthropods beginning 559 MYA			
563	Phylum: Arthropoda	Segmented body with an exoskeleton	
563	SubPhylum: Chelicerata	2 part body plan with appendages anterior to the mouth	
559	Class: Merostomata	Limulus polyphemus (horseshoe crab; Y)	2 are Tsg[e]
559	Class: Arachnida	Tetranychus urticae (spider mite; Y)	1 is Tsg
563	Clade: Mandibulata	2 modified limbs used in food processing	
518	SubPhylum: Crustacea	Primarily aquatic with biramous limbs	
518	Class: Branchiopoda	Daphnia magna (water flea; Y)	1 is Tsg
518	Subphylum: Hexapoda	Insects (3 part body plan and 3 pairs of legs)	
459	Class: Collembola	Folsomia candida (springtail; Y)	1 is Tsg
459	Class: Insecta	body plan has wings	
401	Superorder: Palaeoptera	Ladona fulva (dragonfly; Y)	1 is Tsg
383	Superorder: Polyneoptera	Schistocerca gregaria (grasshopper; Y)	1 like Tsg
383	Superorder: Paraneoptera	Aphis gossypii (cotton aphid; Y)	1 is Tsg
383	Superorder: Endopterygota	Holometabolous (distinct larvae, pupae and adults)	
344	Order: Coleoptera	Tribolium castaneum (red flour beetle; Y)	1 is Tsg
344	Order: Hymenoptera	Apis mellifera (european honey bee; Y)	1 like Tsg
		Nasonia vitripennis (parasitoid wasp; Y)	2 are Tsg[e]
267	Order: Neuroptera	Chrysoperla carnea (green lacewing; Y)	1 is Tsg
246	Order: Lepidoptera	Bicyclus anynana (brown butterfly; Y)	1 is Tsg
		Bombyx mori (silk moth; Y)	1 is Tsg
344	Order: Diptera	Flies (one pair wings and one pair halteres)	
256	Suborder: Nematocera	Elongated flies with aquatic larvae	
		Anopheles darlingi (american mosquito; Y)	2 are Tsg[e]
		Phlebotomus papatasi (sandfly; Y)	1 like Tsg
III. Cv appears in the fruitfly lineage (Brachycera) roughly 256 MYA			
256	Suborder: Brachycera	Non-elongated flies with reduced antennal segments	
129	Clade: Calyptratae	Musca domestica (house fly; Y)	1 is Tsg;2 are Cv
		Lucilia cuprina (greenbottle fly; Y)	1 is Tsg;2 are Cv
129	Clade: Acalyptratae	Lacking posterior wing lobes analogous to anterior alula	
61	Tribe: Colocasiomyini	Scaptodrosophila lebanonensis (vinegar fly; Y)	1 is Tsg;1 is Cv
61	Tribe: Drosophilini	Zaprionus bogoriensis (white striped body; Y)	1 is Tsg;1 is Cv
IV. Shrew appears in the Drosophila genus roughly 43 MYA			
43	Subgenus: Hawaiian	Drosophila griimshaw (Y)	1 each Tsg, Cv, Srw
43	Subgenus Drosophila	Drosophila hydei (Y)	1 each Tsg, Cv, Srw
		Drosophila virilis (Y)	1 each Tsg, Cv, Srw
	Subgenus: Sophophora	Drosophila melanogaster (Y)	1 each Tsg, Cv, Srw

a. Dates from www.Timetree.org
b. Linnean Rank from NCBI Taxonomy Browser
c. Status from NCBI Genome - see Table S1 for details
d. Tsg family members and their fly homologs (is) or fly nearest relative (like) are shown by neighbor joining trees or if that is insufficient then shown via pairwise BLASTp "align two"
d. Recent duplication very similar to each other like BMP2/BMP4; not present in related species

two' analyses and clarifies the annotation of all three as Tsg. Unlike Srw, both Musca Cv-like proteins retain the BMP binding domain. However, since Srw is closer to Cv than Tsg in D. melanogaster (Fig. S4), a duplication of Cv is a necessary precursor to Srw.

In the superfamily Acalyptratae leading to Drosophila, there appear to be two trajectories for the Tsg family. First, in two subfamilies that diverged from *D. melanogaster* 61 mya the Cv-like duplicate is lost and there are only Tsg and Cv. These subfamilies are the Colocasiomyini (vinegar fly) and the Drosophilini (white striped body fly) that share numerous characteristics with *D. melanogaster* (Li et al., 2022). The second trajectory is seen in the subgenus Drosophila, where we examined over a dozen fully sequenced species. We found three Tsg family members in all: Tsg, Cv and Srw. For example, *D. grimshawi* (43 mya; (Throckmorton, 1975) contains a Srw protein missing its amino terminal BMP-binding domain that matches *D. melanogaster* Srw in our 'align two' analysis. Overall, we infer that Srw originated at a timepoint between the *D. melanogaster* relatives that diverged 61 mya (e.g., Zaprionus) and the diversification of the subgenus Drosophila 43 mya (e.g., D. grimshawi). During this window of 18 million years one of the two Cv proteins lost its BMP binding domain and was neofunctionalized to create Srw.

Presence of Srw correlates with accelerated embryonic development

Given the limited taxonomic distribution of Srw, our hypothesis was that it arose due to strong selective pressure for adaptations that accelerate Drosophila embryonic development. This hypothesis originates in the view that minimizing immobile developmental stages such as the egg reduce the individual's exposure to predation, parasitism, and environmental stress (e.g.,(Hermann et al., 2019; Zalucki et al., 2002). While far fewer species have embryonic duration than genome sequence data, there are enough within Insecta to test the prediction that Srw is present only species with the shortest time to gastrulation and hatching. We began by examining the species having Tsg alone (Table 3). This group includes several developmental model organisms that show a range of 'time to gastrulation' between 11 hours (beetle and mosquito) and 96 hours (dragonfly). Among these species, the one with the longest time to gastrulation (dragonfly) does not have with the longest embryonic stage (longest is 42 days;

aphid). Importantly for the hypothesis test, the species with the shortest time to gastrulation (beetle and mosquito) also have the shortest time to hatching (3 and 2 days respectively).

Table 3. Tsg family in Insect: Srw correlates with reduced time to gastrulation

Taxon	Characteristics: exemplars	time to gastrulation (example)[a]	duration embryo
Tsg			
Insecta	Hemimetabolous usually 2 pairs of wings		
Palaeoptera	Cannot fold wings: Dragonfly, Mayfly	96 hours (Ischnura)	10 days
Polyneoptera	Sound producing: Cricket, Grasshopper	48 hours (Schistocerca)	14 days
Paraneoptera	Sucking mouthparts: Aphid, Lice	48 hours (Acyrthosiphon)	42 days
Endopterygota	Holometabolous (full metamorphosis)		
Coleoptera	Armored forewings: Beetle, Weevil	11 hours (Tribolium)	3 days
Hymenoptera	Social insects: Ant, Bee, Wasp	30 hours (Apis)	3 days
Neuroptera	Many wing veins: Lacewing, Spoonwing	(Chrysoperla)	4 days
Lepidoptera	Scales on body & wing: Butterfly, Moth	24 hours (Bombyx)	7 days
Diptera	Halteres replace hindwings		
Nematocera	Body parts elongated: Mosquito, Sandfly	11 hours (Anopheles)	2 days
Tsg+Cv			
Brachycera	Reduced antennal segmentation		
Calyptratae	Wing covers halteres: House fly, Blow fly	4 hours (Megaselia)	29 hours
Colocasiomyini	Crop pest fruit flies: Oriental fruit fly	8 hours (Bactrocera)	42 hours
Drosophilini	White striped body: African Fig fly	(Zaprionus)	1 day
Tsg+Cv+Srw			
Drosophila	Non-pest fruit flies		
Hawaiian	>600 endemic species	(grimshawi)	6 days
Drosophila	Includes 16 cactophilic species	4 hours (virilis)	26 hours
Sophophora	311 species worldwide	3 hours (melanogaster)	22 hours

a. Sources top to bottom: Simon et al. 2017; Deardon & Akam 2001; Lin et al. 2014; Benton et al. 2013; Fen et al. 2019; Souza et al. 2016; Nakao 2021; Goltsev et al. 2009; Disney 2008; Anderson 1972 (synonym Dacus); Pfeiffer et al. 2019; Ken Kaneshiro personal communication; Wotton et al. 2014; Chong et al. 2018 and Calderon et al. 2022.

Sources alphabetical: (Anderson D, 1972; Benton et al., 2013; Calderon et al., 2022; Chong et al., 2018; Dearden and Akam, 2001; Disney, 2008; Fen et al., 2019; Goltsev et al., 2009; Nakao, 2021; Pfeiffer et al. 2019; Simon et al., 2017; Souza et al., 2016; Wotton, 2014).

In species that have Tsg and Cv, the second family member does not facilitate short developmental times. For example, in *Bactrocera dorsalis* (oriental fruit fly) embryos take 8 hours to gastrulate and 42 hours to hatch. In species with Tsg and 2 Cv proteins such as *Megaselia abdita* that has a mechanism of D/V patterning like *D. melanogaster* (Kwan et al., 2016; Rafiqi et al., 2012), there is evidence of selection for rapid embryogenesis. This species displays developmental timing that is roughly equal to *D. virilis*, a species that contains Srw (4 hours to gastrulation and 29 hours to hatching) (Schmidt-Ott and Kwan, 2022).

In Drosophila, where all species examined have Srw, *D. melanogaster* displays a time to gastrulation and time to hatching are the shortest among insects at 3 hours to gastrulation then 22 hours to hatching. Slower Drosophila species, diverging after the creation of Srw may have developed other adaptions to predation on eggs, such as choice of oviposition site, chorion strength, or increased female fecundity (Markow, 2015). Overall, the data is consistent with the hypothesis that selection for efficiency in embryonic D/V axis formation resulted in the generation of Srw from a copy of Cv, by truncation and reframing its function as an embryonic developmental accelerator.

Discussion

Patterning the dorsal tissues of the Drosophila embryo requires BMP signaling and an additional set of interacting components that modify the distribution and activity of the BMP ligand in time and space. These factors include the BMP binding proteins Sog and Tsg, the metalloprotease Tld and components of the extracellular matrix (Matsuda et al., 2016; Sawala et al., 2015; Upadhyay et al., 2017; Wang et al., 2008). Together, these factors enable net shuttling of the BMP ligand to the dorsal-most region generating a highpoint of signaling activity. Computational models provided insights into the biophysical properties necessary to produce the experimentally observed patterns within the short three-hour time frame before dorsal cell fates are established and gastrulation commences (Eldar et al., 2002; Shimmi et al., 2005b; Umulis et al., 2006; Umulis et al., 2010). Homologous proteins perform similar functions to establish BMP activity gradients in several types of vertebrate embryos, but expression and interactions among the different components result in unique patterning solutions appropriate for the geometry and developmental period of their embryos (Madamanchi et al., 2021; Mörsdorf et al., 2024).

Among the remarkable sequence conservation of BMP associated patterning molecules across evolutionarily distant species, Srw stands out as an exception. Srw is an N-terminal truncated relative of Tsg (Bonds et al., 2007) that has not been described in vertebrates or in

insects outside the genus Drosophila. In this report we decipher the evolutionary origin of Srw and examine some of its biochemical properties.

Developmental timing is considered a key phenotypic trait with large effects on the Darwinian fitness of a species. In many insects, developmental time is constantly under strong selection pressure to minimize the duration of the most vulnerable stages, immobile eggs and pupae. However, the genetic/molecular changes that underlie adaptations in species-specific responses to selection for reduced time are poorly understood. Here we provide evidence that selection pressure for efficiency in embryonic D/V patterning impacted Srw, the newest gene in the Tsg family. This pressure led to the loss of the BMP binding domain in Srw and its neofunctional role in D/V patterning as an accessory that serves to accelerate Sog cleavage by Tld, leading to the relatively rapid generation of maximal Dpp signaling at the dorsal midline.

Several alternative hypotheses for Srw function can be envisioned. One is that since *D. melanogaster* D/V patterning is dependent on Dpp-Scw heterodimers (Shimmi et al., 2005b), it is possible that Srw arose to accommodate the Dpp-Scw heterodimer. Dpp-Scw heterodimers are a recent innovation as they are not the D/V patterning ligand in Deuterostomes (Oelgeschläger et al., 2000) and non-Brachycera insects such as Tribolium (Nunes da Fonseca et al., 2010). The prediction is that Scw and Srw will co-exist in most or all species where Scw is present, although the hypothesis presumes Scw arose first. To assess this hypothesis, we took the most conserved portion of Scw, the cystine knot region of the ligand (Wisotzkey and Newfeld, 2020) and examined each of the species shown in Table 2. We took special care in the analysis of the mosquito and sandfly in the Nematocera, sister Suborder to the Brachycera. There is no evidence of Scw in any of these species. Interestingly in the Brachycera where Cv first appears, so does Scw. This includes the house fly, green bottle fly, vinegar fly and all Drosophila plus the blow fly from Table 3. The exception is the white striped body fly where Scw appears to have been lost, like Tsg in C. elegans. Thus, the alternative hypothesis does not hold since Scw existed for nearly 200 million years before the advent of Srw between 61 and 43 mya. We conclude that Srw did not evolve to accommodate Dpp-Scw heterodimers.

An alternative hypothesis for Srw origin includes the accelerator mechanism with a distinct selective pressure. Instead of responding to pressure for a reduced D/V patterning period, the pressure is to accommodate increasing D/V distance in larger eggs. The prediction is that increased D/V distance as a proportion of egg length would correlate with species where Srw is present. To assess this prediction, we extracted egg D/V distance (reported as width), and aspect ratio (length/width) from a public dataset of egg size (eggdataset.tsv; (Church et al., 2019a). One conclusion from that analysis was that insect egg size does not co-evolve with developmental timing (Church et al., 2019b). This conclusion suggests that if our timing hypothesis is true, then the alternative D/V length hypothesis cannot also be true. Further, their dataset on developmental timing also shows that *D. melanogaster* has the shortest time to gastrulation of 38 insect species reported (development.tsv; Church et al. 2019a}. We analyzed each of the species shown in Table 3, if present, or their closest phylogenetic relative. If a species were present multiple times (e.g., *Tribolium castaneum*), then we calculated an average for each of the two measures to better capture the range of variation. The data showed that the presence of Srw does not correspond to the insect species with the smallest aspect ratio. Note that at an aspect ratio of 1, eggs are spheres with their width equaling their length}. The three Drosophila species with Srw have oval eggs with aspect ratios of 2.722 (melanogaster), 3.294 (virilis) and 3.375 (picticornis). In contrast, Anopheles (2.212), Bombyx (1.192) and Tribolium (1.935), that do not have Srw, have rounder eggs with greater relative D/V distance. Thus, the hypothesis that Srw was turned into an accelerator by pressure to accommodate greater D/V distance also appears to be false.

It is notable that a Musca egg with a larger aspect ratio (4.364) and thus smaller relative D/V distance, but a greater absolute D/V distance as a result of being 3.7-fold larger than a *D. melanogaster* egg has rapid embryonic development with gastrulation reached in roughly 4 hours. Although this species does not have a copy of Srw, it does have one Tsg and two Cv proteins. One can speculate that the extra Cv began neofunctionalization to accelerate D/V patterning but has not yet experienced the loss of the BMP binding domain that produced Srw in

Drosophila. In this regard, it would be interesting to determine the expression profiles of each Musca Tsg-like protein to see if more than one is expressed at the blastoderm stage.

To our knowledge the adaptation giving rise to Srw would be the first case of a specific genetic response to natural selection on immobile eggs that impacts the duration of D/V axis formation. Interestingly there is a recent report describing a laboratory selection experiment for fast embryonic development employing a wild population of Tribolium. However, in this case, the selected alteration advanced the embryonic ecdysone peak that induces dorsal closure, a process that occurs after D/V patterning. This report also showed that the selected mutation has a negative effect later in life, a reduction in female fecundity (Cheng et al., 2024). To date we have not identified any drawbacks associated with the existence of Srw.

One key biochemical finding relevant to our timing adaption hypothesis is that Srw enhances the cleavage of Sog by Tld, when in a complex with Dpp. This is also a property of high levels of Tsg and its vertebrate relatives, in tissue culture experiments (Scott et al., 2001; Shimmi and O'Connor, 2003; Xie and Fisher, 2005). That Tsg and Srw can both stimulate Sog cleavage by Tld fits well with our rescue data, both positive (Tsg rescues *srw*) and negative (Srw does not rescue *tsg*). This observation is also consistent with Tsg, and its vertebrate homologs, having the ability to bind BMPs *via* their N-terminal module that is absent in Srw.

These observations lead to the key question of how Srw and Tsg accelerate Tld catalysis of Sog proteolytic cleavage and how this might fit with *srw* phylogeny. Since we can detect no strong association of Srw with any known D/V pattering component or complex by Co-IP analysis, a model for Srw function should be consistent with the apparent weak/transient nature of Srw interaction with other D/V patterning components. The simplest model is that Srw, or the C-terminal domain of Tsg, might transiently interacts with Tld, perhaps through a Tld CUB repeat (a heterodimerization interface), to enhance its proteolytic activity at Sog cleavage sites.

To our knowledge there is no precedent for this model in the literature although Procollagen C-protease enhancers (PCPE-1 and 2) stimulate BMP1/Tld and other Tld-related enzymes to process substrates besides Sog/Chordin, including several types of procollagens

(Moali et al., 2005). However, PCPE-1 appears to function by binding to the collagen substrate to alter its availability to the protease rather than interacting with the protease itself. In addition, using AlphaFold, we could not find any predicated interaction sites between Srw and Tld.

The model that we favor (Fig. 6) is consistent with both the putative selective pressure that led to a new adaptation via Srw truncation from a second Cv protein, and the ability of Tsg to rescue Srw mutants if excess Tsg is supplied. It is a modification of a previously proposed model and incorporates all known biochemical associations between the various components including Collagen IV, BMPs, Tsg and Tld. In these previous reports, the authors demonstrate that the Dpp-Scw heterodimer can bind to an N-terminal motif found in Drosophila type IV Collagens present in the early embryo extracellular matrix and that Sog can also be assembled with the BMP bound to collagen (Sawala et al., 2012; Wang et al., 2008; Winstanley et al., 2015). Furthermore, Tld can associate with collagen via CUB domains 1-3 and with Sog via CUB 4 and 5 and mutations in these CUB repeats alter cleavage of Sog by Tld (Winstanley et al., 2015). A hypothetical schematic representation of this matrix associated complex is shown in Fig 6.1, although the order of its assembly is not known.

A key observation was that addition of Tsg to a reaction mix containing this complex displaced the Sog/BMP heterodimer complex from collagen, enabling Tsg to assemble into a multimeric complex through two associations: one with a BMP through its N-terminal BMP binding domain, and a second with a Sog VWF domain via its C- terminal Srw-like domain (Malinauskas et al., 2024; Wang et al., 2008; Winstanley et al., 2015). This displacement-integration process was found to stimulate Tld cleavage of Sog.

We suggest that while Tsg can provide this function *in vitro*, perhaps its *in vivo* ability to displace, integrate and stimulate Sog cleavage is sterically hindered, thus requiring a high level of Tsg. We further postulate that Srw, via a transient interaction with a Sog VWF domain, similar to that recently described for Tsg interactions with a Sog VWF (Moore et al., 2025; see Fig 2) could be the collagen displacing component that enables Tsg to associate into a stable complex via its N-terminal domain binding to a BMP and its C-terminal Srw-like domain

binding to a Sog VWF. This stable binding is hypothesized to lock in a conformational change enabling the Tld metalloprotease to more efficiently initiate cleavage of Sog at the three cleavage sites. If Srw is not present, then Tsg can do the job but requires a higher concentration to stimulate collagen displacement and assembly into the Tld containing complex. The results of our chimeric rescue experiments are consistent with this model. The Tsg-Srw chimera that contains the Sog VWF domain can rescue *srw* mutants at low but not high mRNA concentrations. We propose that at high concentrations, the chimera acts as a dominant negative with respect to the endogenous Tsg since the Srw C-terminal tail in the chimera is short and therefore may not be able to assemble into a stable complex with Sog. This also explains why the chimera does not rescue *tsg* mutants either since it cannot make a stable association with Sog. In contrast, the Tsg-SrwΔ chimera has neither a long C-terminal tail nor the Sog VWF binding domain, thus no productive interactions with Sog and does not rescue *tsg* or *srw* mutants.

While numerous variants of this scheme can be envisioned, the model can explain an unusual aspect of *srw* genetics. Although there is significant similarity in the phenotypes of *tsg* and *srw* mutants consistent with some overlap in biochemical function, the genetic epistasis tests clearly indicate that there is some difference between the two. Specifically, we find that Tld function is epistatic to Srw while in a previous report it was shown that Tsg function was epistatic to Tld (Shimmi and O'Connor, 2003). This is consistent with the proposed model. In the case of *tsg* mutants, no stable inhibitory, shuttling complex can form. As a result, Tld function is irrelevant and there is a low level Dpp-Srw signal throughout the dorsal domain in both *tsg* and *tsg, tld* double mutants. In contrast, in *srw* mutants the Tsg and Sog complex likely forms at some rate and, although the kinetics are slow, Tld can process this complex, the result being that shuttling does not proceed at the proper rate leading to a n expanded low Dpp-Scw signal. In the double *srw, tld* mutant, however, there is no cleavage and even though the rate of formation of the inhibitory complex is slow in the absence of Tld, it likely builds up over time and ultimately leads to complete inhibition of signaling. Future biochemical and genetic investigation will be needed to confirm this model.

Materials and Methods

Molecular Genetics

Fly stocks

The following lines are available at the Bloomington Drosophila Stock Center *w[1118]* (RRID:6326), *tld^{B4}/TM3, hb-LacZ, Sb,Ser* (RRID:5396). The *sog^{YL26}, tsg^{XB86}, srw^{1} and srw^{10k}* alleles were from Christiane Nusslein-Volhard and were rebalanced over FM7, *ftz-LacZ* or *TM3, Sb ftz-LacZ*. The *srw^{B3}, srw^{B4}, srwB^{18}*, alleles were obtained from Chip Fergusion (Ferguson and Anderson, 1992b) and rebalanced over *TM3, Sb ftz-LacZ*. The *srw $^{h2.19}$, srw$^{15.33}$, srw$^{110.18}$, srw$^{65.46}$, srw$^{75.41}$, srw$^{34.67}$, and srw$^{104.20}$* alleles were obtained from Ruth Lehmann and similarly rebalanced.

Identification of the srw locus and transcript

At the turn of the century, after two steps of chromosome walking beyond the end of BAC(D471) using λ fix genomic library screens, we arrived near the *srw* locus concurrent with the release of the Celera sequence extending ~60 kb beyond BAC(D471) (Genbank: AC019525). Theorizing that *srw* would have some homology to *tsg* and a large hydrophilic ORF, we utilized BLAST to narrow down the putative *srw* region then designed primers that would include the region of interest. PCR showed an amplified region of 480 bps was on 3 of the λ phages from the walk (λ7, λ10, λ11) as well as in wild type Drosophila genomic DNA. The *srw* transcript was also identified via these primers in 0–4-hour, 4-8 hour, and 12–24-hour Nick Brown cDNA libraries (Brown and Kafatos, 1988). cDNAs and genomic PCR products were the same size suggesting that any introns would be small. Sequencing of 12 *srw* mutants (Table 1) verified the identity of this gene as *srw*. To define the functional limits of the *srw* locus, we designed transgenes to rescue the *srw* mutant phenotype. A 6.7 kb BamHI fragment from λ10 was inserted into *pCaSpeR4* (Drosophila Genomics Resource Center RRID:1213) yielding pMBO2145. Transgenic lines with this plasmid, designated P(*Casper*-genomic *srw*), were able to rescue transheterozygous mutant *srw^{B4} / srw^{B18}* flies. To create an epitope tagged Srw rescue transgene, the genomic *srw* fragment was reassembled with the 6XHis C-terminal tag of pMBO2156 in the

pCaSpeR4 vector (pMBO2197). Transgenic lines P(*Casper*-genomic *srw 6XHis)* rescued transheterozygous *srw* mutants, showing that C-terminal tagging of Srw does not affect function.

Isolation of a srw cDNA

The *srw* cDNA was obtained using the MACH method (Haerry and O'Connor, 2002) from the 0-4 hour Nick Brown library. In brief, tail-to-tail divergent primer pairs to two different parts of the *srw* gene were employed to with the 0-4 hour cDNA library as template yielding both strands of the entire plasmid containing the *srw* cDNA. After DpnI digestion, the two strands were isolated, annealed to each other utilized to transform *E. coli*. Positive clones, named pMBO2153, were sequenced to verify the start of the *srw* gene, confirm the absence introns, and that our genomic isolates contained the entire *srw* locus.

Tagging the srw cDNA with 6XHis and 3XHA

A ~450 bp *srw* fragment that should include the entire open reading frame (ORF) flanked by Asp718I and XbaI sites, was PCR amplified from the λ11 genomic template, cut with Asp718I and XbaI and ligated into the Asp718I and XbaI sites of *pBluescript II KS+* (pMBO2152, pBS-*srw)*. Annealed primers of the top and bottom strands of 6XHis were ligated into the XbaI site to generate pMBO2156 (pBS-*srw*-6XHis). For S2 cell culture expression, the Asp718I-XbaI fragment of pMBO2156 was ligated into Asp718I-NheI sites of *pBRAcPA* (*pBR322-actin5C promoter-sv40 poly A*; (Angelichio et al., 1991) to generate pMBO2162 (AcPA-*srw*- 6XHis).

The same XbaI site of pMBO2152 was blunt ended with the Klenow enzyme and employed to clone the ~250bp fragment of 3XHA (Tyers et al., 1992) that had previously had its SacI end blunted by exonuclease activity and the XbaI end filled in by Klenow. The resulting plasmid pMBO2201 (pBS-*srw*-3XHA) was sequence verified for the correct orientation of 3X HA and retention of the ORF. *srw-3XHA* was sequence verified and encodes the following protein: MKTLLTIYILLSFGELGLANMAQMRKKSHTEEFEGMPALFRAMSSSPNDGYTY NWSVVSFSTNGKPGSGLNCTVLYLDQCTSWNKCRQTCLKTGATSYRWFHDGCCECVG ELCMNYGVNESRCRLCPEPGLEDEDD**DEWGYGEEDEFSSSYPYDVPDYAGYPYDVPD YAGYPYDVPDYA***

Tagging the tsg cDNA with 3XHA

The re-assembled *tsg* cDNA with an XbaI site at the C terminus was ligated with the annealed top and bottom strands of 3XHA, as was described for 6XHis above, to yield pMBO2411. *srw-3XHA* was sequence verified and encodes the following protein:

MQLLCYFVILFVGIAPWSSLANDDGCNEVVCGSVVSKCLITQSCQCKLNDCHC
CKDCLNCLGELYIECCGCLDMCPKHKDVLPSLTPRSEIGDIEGVPELFDTLTAEDDEGWS
TIRFSMRAGFKQRVQGGASGDAGNGNGNGNAGSAGVTLCTVIYVNSCIRANKCRQQCE
SMGASSYRWFHDGCCECVGENCLNYGINESRCRGCPEDQDQLLTADTVPAEAEQDLER
FFGNEEIE**DEWGYGEEDEFSSSYPYDVPDYAGYPYDVPDYAGYPYDVPDYA***

Construction of Tsg-Srw chimeric proteins

The N terminal domain of Tsg was inserted upstream of either the entire *srw* gene, excluding the signal peptide (Tsg-Srw), or the C terminal "half" of the Srw gene starting at the first conserved cysteine residue (TsgΔSrw). These chimeric proteins were placed in the SP64TBX (Promega) vector for RNA injection experiments.

1) Tsg-Srw chimera sequence: **Bold = Srw**

MQLLCYFVILFVGIAPWSSLANDDGCNEVVCGSVVSKCLITQSCQCKLNDCHCCKDCLN
CLGELYIECCGCLDMCPKHKDVLPSLTPRSEIGDIEGVPELFDTLTAEDDEGWSTIRFSMR
AGFKQRVQGGASGDAGNGNGNGNAGSA**NMAQMRKKSHTEEFEGMPALFRAMSSSP**
NDGYTYNWSVVSFSTNGKPGSGLNCTVLYLDQCTSWNKCRQTCLKTGATSYRWF
HDGCCECVGELCMNYGVNESRCRLCPEPGLEDEDD

2) TsgΔSrw sequence: **Bold = Srw**

MQLLCYFVILFVGIAPWSSLANDDGCNEVVCGSVVSKCLITQSCQCKLNDCHCCKDCLN
CLGELYIECCGCLDMCPKHKDVLPSLTPRSEIGDIEGVPELFDTLTAEDDEGWSTIRFSMR
AGFKQRVQGGASGDAGNGNGNGNAGSA**CTVLYLDQCTSWNKCRQTCLKTGATSYR**
WFHDGCCECVGELCMNYGVNESRCRLCPEPGLEDEDD

Preparation of mRNA for injections and analysis of injected embryos

Capped mRNA for microinjection was generated using the mMessage mMachine T7 kit

(Ambion; Cat#1344). Dechorionated embryos were prepared as described previously (Ferguson and Anderson 1992, Nguyen et al., 1998), with the following modifications. Embryos at the pre-cellular blastoderm stage were injected by inserting the needle laterally and delivering approximately 34 picoliters (pl) of the indicated mRNAs using a programmable microinjector (Narishige IM-300). Following injection, embryos were incubated in a humid chamber at 18°C until stage 14, then fixed in glutaraldehyde-saturated heptane for 4 minutes. After fixation, embryos were manually removed from the vitelline membrane and incubated in X-Gal activity staining solution at 22°C for 16 hours to visualize the *Kr-LacZ* reporter that is expressed in amnioserosa cells. *srw* mutant embryos were identified by the absence of a *Ubx-LacZ* reporter located on the III chromosome TM3 balancer, while *tsg* mutant embryos were identified by the absence of a *ftz-LacZ* marker located on the X chromosome balancer FM7c (Parvy et al. 2005).

In situ hybridizations

Sense and anti-sense strands of digoxigenin-labelled *srw*, *rho*, *sog*, and *dpp* (made from cDNA clones in pNB40) were hybridized to early wild type (w^{1118}) and mutant embryos aged 0-6 hours after egg lay as described by in (Shimell et al., 1991). Only embryos probed with the *srw* antisense strand displayed expression. To unambiguously identify mutant embryos, a *lac Z* antisense probe was included that hybridized to the balancer derived *LacZ* gene.

Immunohistochemistry

Embryos were collected, dechorionated, fixed and devitellinized as described (Mitchison and Sedat, 1983). Embryos were incubated overnight at 4°C in phosphate buffered saline (PBS) plus .1% Tween 80 (PBT) with a primary antibody (1/1000 α-pMad, gift from Peter ten Dike, 1/1000 α-LacZ , Promega), 1/100 α-Kr, gift from Claude Desplan) and then washed 4X for 30 minutes in PBT and incubated for 2 hours with appropriated secondary antibody (rabbit α-DIG 1/1000 or α–HRP Vectorstain Elite ABC kit, Vector Labs). After 2X washes for 1 hour each in PBT color development was carried out according to the manufacturer's directions.

Srw 6XHis transfections

Drosophila S2 cells were transfected with AcPA-*srw* 6XHis DNA using DDAB (Avanti

Cat#890810P) and cultured in Shields and Sang M3 insect medium (Sigma Cat#S89398) with 10% insect medium supplement (Sigma Cat#I7267). After 5 days, cells were physically dislodged, gently spun down, and the supernatant employed in cleavage reactions.

Cleavage reactions

Transfection and culturing of S2 cells has been described (Yu et al., 2000). For cleavage reactions, the components were: 1) Sog-Myc (purified protein; O. Shimmi), Tld-HA (supernatant; transiently transfected S2 cells), 2) ligand in various forms (Dpp-HA or Scw-HA supernatants or recombinant Dpp; R&D Systems Cat#159-DP), 3) Tsg-His (purified protein; O. Shimmi), and 4) Srw-His (purified protein or supernatant from transiently transfected Srw-His cells). Conditions for cleavage reactions and Western blots were described in (Shimmi and O'Connor, 2003).

Transgenes for expression in the female germline

The plasmid pUAS-K10attB was used as the vector for expression of Srw or Tsg in the female germline (Koch et al., 2009). Specifically, a 645 bp fragment was PCR amplified using *Sfi srw 02for* and *Xba srw 02rev* primers on pMBO2201 that contains the *srw* coding sequence (CDS), *3XHA* tagged in pBluescript II KS+. The PCR product was digested with SfiI and XbaI, gel purified and ligated into the SfiI and XbaI sites of pUAS-K10attB. Positive clones were sequenced using *srw ORF for* and *srw ORF rev* primers and named pMBO2816. The 900 bp *XbaI-Asp718I* fragment of *tsg-3XHA* was obtained from pMBO2411 (the *tsg* CDS, *3XHA* tagged in pBluescript II KS+), gel purified and ligated into the *XbaI* and *Asp718I* sites of pUAS-K10attB. A positive clone was sequenced and designated as pMBO2817.

PhiC31 mediated integration and creation of UAS; srw mutant stocks

The plasmids pMBO2816 and pMBO2817 were injected into *y[1] w[1118]; PBac(y[+]-*

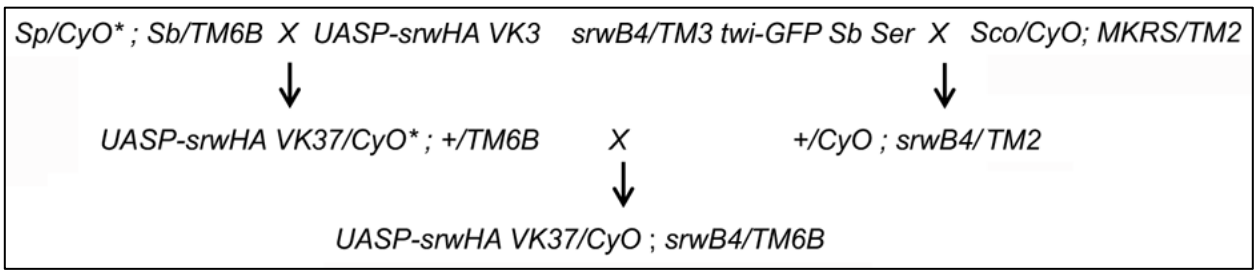

attP-3B)VK00037 (BDSC#9752, BestGene) using PhiC31 integration. These flies were given the shorthand names of *UASP-srwHA VK37* and *UASP-tsgHA VK37.* UAS Srw homozygous; srw^{B4} balanced stocks were obtained via the following strategy:

These stocks were crossed to a complementary stock with Gal4 and a different *srw* allele to drive UAS expression in transheterozygous *srw* mutant offspring.

UASP-srwHA VK37; srwB4/TM6B or UASP-tsgHA VK37; srwB4/TM6B

UASP-srwHA VK37; srwB18/TM6B or UASP-tsgHA VK37; srwB18/TM6B

Table 4. Plasmids

pMBO number	Shorthand name	Use
2145	CaSpeR-genomic *srw*	Genomic rescue
2197	CaSpeR-genomic *srw* 6XHis	Genomic rescue
2153	NB40-*srw* cDNA	*In situ* probes
2411	pBS-*tsg* 3XHA	intermediate
2152	pBS-*srw* cDNA	intermediate
2156	pBS-*srw* 6XHis	intermediate
2201	pBS-*srw* 3XHA	intermediate
2162	AcPA-*srw* 6XHis	Cell culture
2816	UAS-K10 attB-*srw* 3XHA	PhiC31 integration
2817	UAS-K10 attB-*tsg* 3XHA	PhiC31 integration
2315	SP64-dTsg(N)-Srw(Cys rich)	mRNA injections
2316	SP64-dTsg(N)-Srw	mRNA injections

Table 5. Primers

Primer name	Sequence	Use
6XHis TOP	5' CTAGGGGAAGTCATCACCATCACCATCACTAGCT 3'	tagging
6XHis BOT	5' AGCTAGTGATGGTGATGGTGATGACTTCCCCTAG 3'	tagging
Sfi srw 02for	5' TGGCCGCATAGGCCAACACTTCAGTTGCATATTCC	PCR
Xba srw 02rev	5' CTGCTGTCTAGACTCACTATAGGGCGAATTGG 3'	PCR
srw ORFfor	5' GAAAACACTTCTGACTATCTAC 3'	Seq
srw ORFrev	5' CATCTTCATCTTCAAGTCCG 3'	Seq
3X HA stop top	See below	tagging
3XHA stop bot	See below	tagging

Primer 3XHA stop top:

5'CTAGTTACCCATACGATGTTCCTGACTATGCGGGCTATCCCTATGACGTCCCGGAC

TATGCAGGATATCCATATGACGTTCCAGATTACGCTTAGCT3'

Primer 3XHA stop bot:

5’CTAGAGCTAAGCGTAATCTGGAACGTCATATGGATATCCTGCATAGTCCGGGACG

TCATAGGGATAGCCCGCATAGTCAGGAACATCGTATGGGTAA3’

AlphaFold analysis

Predicted structures for Srw (AF-Q9VZE5-F1-modelv4), Tsg (AF-P54356-F1-modelv4), and Cv (AF-Q9W494-F1-modelv4) were obtained from the AlphaFold Protein Structure Database (Jumper et al. 2021, Varadi et al. 2024). Predicted interactions were generated using the AlphaFold Server (Abramson et al. 2024). The reference sequences for Srw (NP_647886), Tsg (NP_511135), and Cv (NP_536786) were our inputs. For visualization and modeling, the signal peptides of Srw (residues 1-18), Tsg (1-20), and Cv (1-25) were removed. To define the equivalent of Chordin VWF-4 in Sog, the protein sequence of Chordin (Q9H2X0) was aligned to Sog (Q24025) via NEEDLE (Madeira et al. 2024). Uniprot defines VWF-4 of Chordin as residues 872-932 (uniprot.org/uniprotkb/Q9H2X0/entry). The VWF-4 domain of Sog was therefore defined as the aligned region in Sog, residues 941-1017. The resulting models were aligned to confirm similarity. Sidechain clashes were visualized employing the show_bumps.py plug-in in Pymol and compared with relaxed models developed with OpenMM/Amber (ColabFold; Mirdita et al. 2022).

Evolutionary Genetics

Identification of species with Tsg family members

To create a Query, the sequence (FASTA format) for each of the three *D. melanogaster* Tsg family members was retrieved from the *D. melanogaster* reference genome in GenBank: 1) Crossveinless (Cv; NP_536786; isoform A - the proteins encoded by three distinct transcripts are identical), 2) Shrew (Srw; NP_647886; isoform B - one transcript and one protein), and 3) Twisted gastrulation (Tsg; NP_511135; isoform A - one transcript and one protein). These were aligned in Clustal Omega with default parameters (ebi.ac.uk/Tools/msa/clustalo). The alignment identified a 57 amino acid region toward the carboxy terminus of each that is common to all three proteins: Cv 166-223, Srw 72-129 and Tsg 140-197. This region contains 9 cysteines and is

66% identical (38/57) across the three proteins. In a control experiment, BLASTp (blast.ncbi.nlm.nih.gov) of this region against the *D. melanogaster* reference genome (NCBI taxonomy ID 6447) returned the three family members, confirming its ability to detect each one.

To identify Subject species there were several steps. First, the detailed version of Lifemap (de Vienne, 2016)https://lifemap-ncbi.univ-lyon1.fr) was employed with Metazoa (multicellular animals) as a starting point. Metazoa was chosen because one of its basal taxa (Phylum Porifera; sponges) contains the earliest known version of the TGF-β pathway (Nichols et al., 2006; Suga et al., 1999). Moving along the Metazoan lineage toward the complex organism *D. melanogaster* allowed the identification of candidate higher taxa to examine (Phylum, Class and Order). Second, a BLASTp search with the Query against each identified taxon was performed to determine if any candidate species with Tsg sequences were present. In some cases, there were none, but for other taxa multiple species were returned. For example, a search of the Phylum Mollusca (taxonomy ID 6447) returned 49 species. Third, species returned by BLASTp were in the NCBI genome database (ncbi.nlm.nih.gov/genome) and the species with the most complete genome sequence (Table S1) in that taxon was chosen for analysis. Verification of lineage and taxon nomenclature for each chosen species was via the NCBI taxonomy browser (www.ncbi.nlm.nih.gov/Taxonomy/Browser/). To place each species into context, their common names and major characteristics were reported from Encyclopedia Britannica (britannica.com). The origin of each taxon in mya was noted in Timetree.org (Kumar et al., 2022). The analysis was completed with available data 11/19/2023.

Identification of Tsg family members in selected species

Sequences were retrieved from individual candidate species by BLASTp with the Query sequence above. All retrieved sequences were downloaded in FASTA format and manually inspected for identical pairs/triplets and for the presence of pairs/triplets differing only by the presence of an amino terminal extension representing an alternatively spliced isoform of the same gene or artifacts of polyA priming when obtained from cDNA rather than genomic DNA. When identical pairs or triplets were noted and only one was from the reference genome (NP or

XP prefix), it was chosen for analysis. In cases where two sequences were not completely identical along their length further analysis was needed to determine if they were variants of the same gene segregating in the population, sequencing errors in reads for the same gene or a recent duplication representing two different genes. We established an empirical threshold for different genes by comparing the reference sequences for mouse BMP2 (NP_031579) and BMP4 (NP_001303289., These are two different genes (chromosomes 20 and 14, respectively) that remain very similar (61% identical over their whole length). The probability associated with the BMP2/BMP4 alignment is $5x10^{-175}$. In our Tsg analysis, any pair with an "align two" probability smaller than that was considered the same gene and only one was moved to phylogenetics.

Phylogenetic analysis of Tsg family members in selected species

We aligned each sequence from all Tsg family members in the selected species, one at a time, with the three *D. melanogaster* family members was created in Custal Omega. Then, for efficiency and because BLASTp had already shown the sequences are clearly similar, a simple Neighbor-joining tree without distance corrections was created in the same program from each alignment. Relationships shown by the alignment, which in a tree of 4 sequences is limited to who is clustered with who versus who is on a branch by itself, established the status of each sequence from the selected species as either Cv, Srw or Tsg.

Identification of gastrulation age and duration of embryogenesis

We conducted an exhaustive literature search, for embryonic development and lifecycle data on insect species representing each of the taxa shown in Table 2. As of 12/15/23, lifecycle data for the duration of the egg stage in a representative species for each taxon was available. Detailed data for embryonic age at gastrulation was available for all but three taxa. In these three cases, corresponding authors reported that gastrulation timing data was not collected.

Acknowledgements

We thank Ken Kaneshiro and Chun Wai Kwan for advice on *Drosophila grimshawi* and *Megaselia abdita* embryonic development, respectively. No competing interests. The Newfeld

lab is supported by NIH R24OD028242. The O'Connor lab is supported by R35 GM118029-09. The Arora lab is supported by UCI endowed chair funds and NIH R01 GM55442. We also thank Osamu Shimmi and Ela Serpe for extensive efforts to identify stable interactions between Srw and other D/V proteins and Aidan Peterson for the western blot showing secretion of Srw-His.

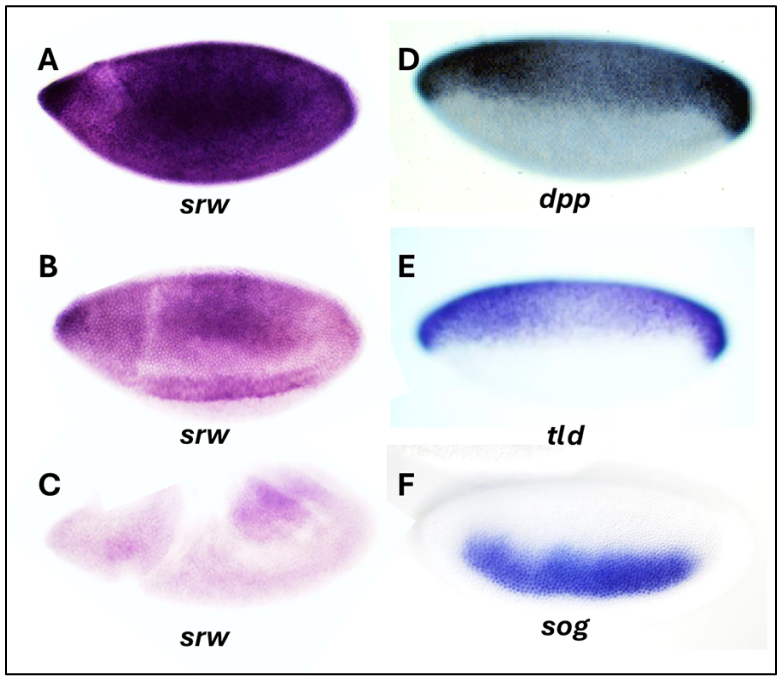

Fig. 1. **Expression of *srw* overlaps with potentially interacting embryonic D/V patterning genes**. A-C) *in situ* hybridization with *srw* antisense RNA probe. A) Late cycle 13 *yw* embryo B) Cycle 14 *yw* early mesoderm invagination embryo. C) Early germband elongation stage *yw* embryo. Note that *srw* expression is dramatically reduced by this stage in comparison to the late cycle 13 embryo. D-F) *in situ* hybridization of yw cycle 13 embryos with D) *dpp* probe., E) *tld* probe, F) *sog* probe.

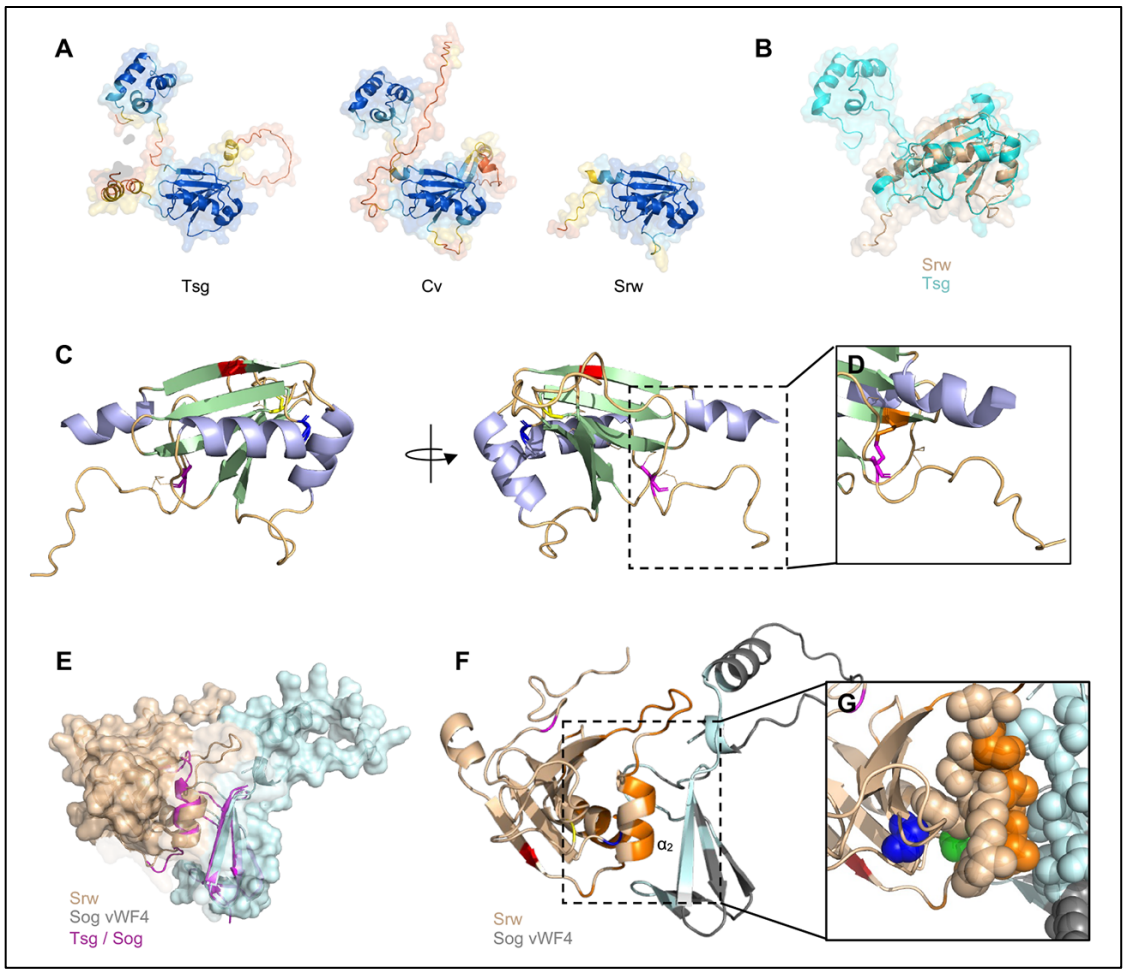

Fig. 2. Srw has a predicted 3D structure similar to C-terminal predictions of Tsg and Cv.

A) AlphaFold structures of Tsg, Cv, and Srw are colored based on a predicted local distance difference test (pLDDT), from high confidence (blue) to low (orange). B) Overlay of Tsg (cyan) and Srw (wheat). Tsg loops (residues 129-145 and 213-249) hidden for clarity. C-D) Ribbon diagram of Srw, colored by secondary structure. Residues G94 (blue), E31 (red), G110 (yellow), and C123 (magenta) are altered in *srw* missense mutations. Their sidechains are shown as stick diagrams. D) Inset: srw^{1} and $srw^{h2.19}$ C123 is predicted to form a disulfide bond with C105 (orange). Together with C80/C126 (lines), these disulfides position the otherwise disordered C-terminus. E) Predicted interaction between Srw (wheat) and Sog VWF-4 (cyan) aligned to the Tsg -Sog prediction (magenta; Moore et al., 2024). F-G) Predicted interaction between Srw (wheat) and Sog VWF-4 domain (grey) with contacting residues highlighted in orange and cyan. Mutants also highlighted. G) Inset: packing of Srw residues against helix 2 next to the VWF-4 beta sheets. Relevant regions shown in space-filling mode. Residues 44-56 hidden for clarity.

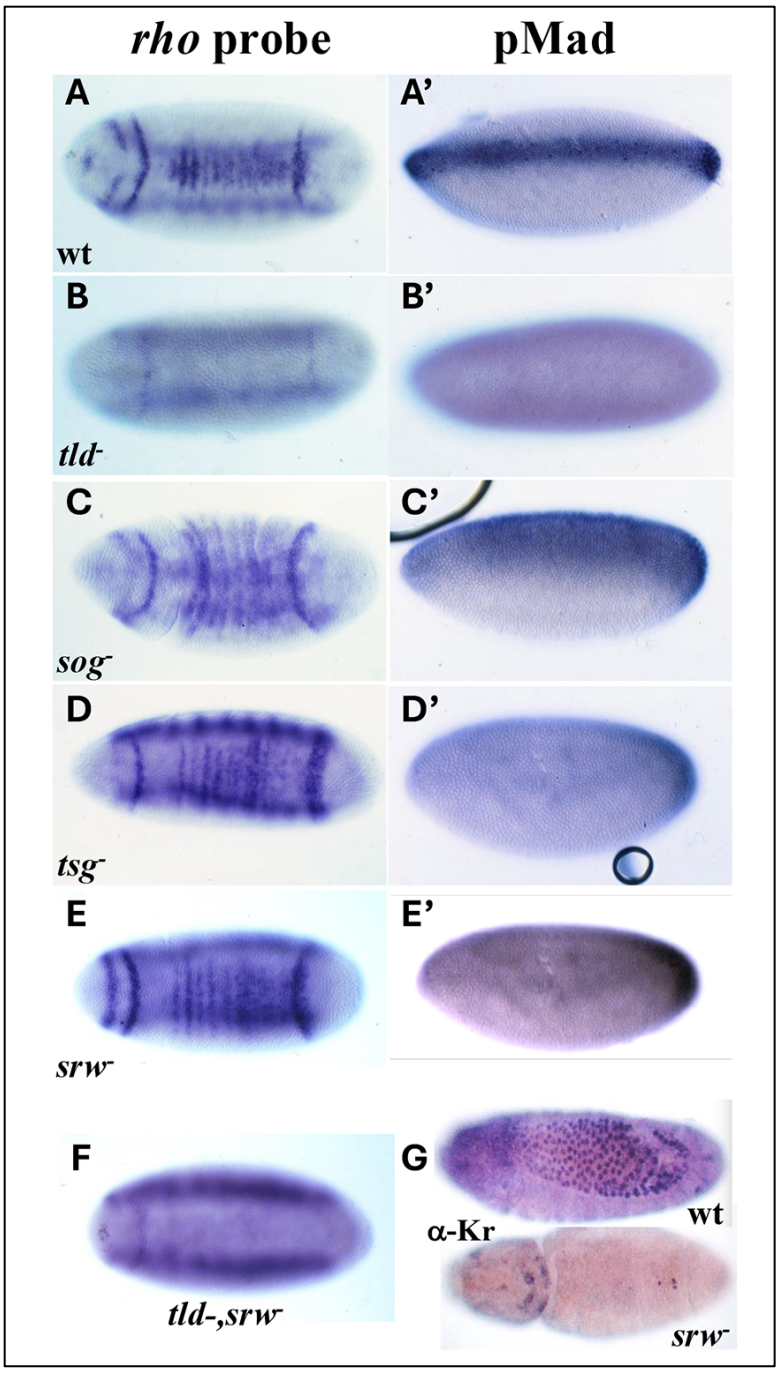

Fig. 3) Mutations in *srw* disrupt D/V patterning and result in loss of amnioserosa cell fate. A- E) In situ hybridization of a *rho* probe to nuclear cycle 13 embryo of the indicated genotypes. The embryos are positioned with the dorsal side oriented pointed towards the reader. A'-E') Nuclear cycle 13 embryos stain with an antibody directed against phosphorylate Mad. The top two panels are also positioned as those in the left column while the bottom three are lateral views. F) A *tld*$^{-}$, *srw*$^{-}$ double mutant embryo hybridized with *rho*. Note the similarity to the tld mutant shown in B sugging that Tld function is epistatic to Srw. G) Top is a wildtype germband retracted embryo showing amnioserosa cells stained with Kr antibody. The panel is a late stage *srw* embryo with no germband retraction due, in part, to the lack of amnioserosa cells.

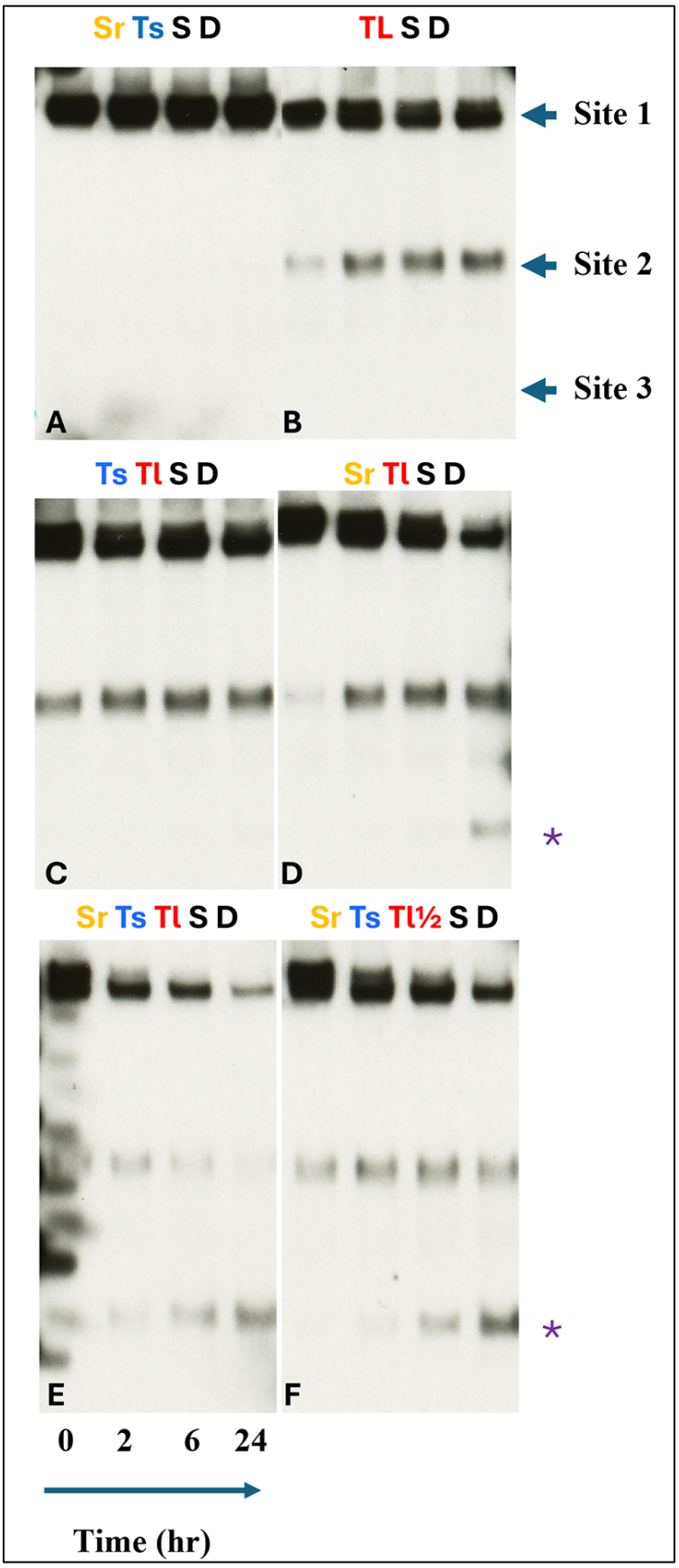
Sr Ts S D
TL S D
Site 1
Site 2
Site 3
A
B
Ts Tl S D
Sr Tl S D
*
C
D
Sr Ts Tl S D
Sr Ts Tl½ S D
*
E
F
0 2 6 24
Time (hr)

Fig. 4. Srw accelerates Tld proteolytic cleavage of Sog. Western blots with anti-HA antibody detecting intact and cleaved forms of Sog-HA. The time course proceeds left to right in the four lanes of A-F and contain reaction aliquots from time zero, 2 hours, 6 hours, and 24 hours respectively. A-F are labeled on top with proteins present in the reactions. S is purified Sog-HA. Ts is purified Tsg. D is purified Dpp. Tl and Sr are predetermined volumes of S2 cell supernatants containing secreted Tld and Srw, respectively. The volume of Tld added was predetermined to be optimal over the specified time course using a defined amount of purified Sog (S) and purified Dpp (D). Tld1/2 denotes a half volume of Tld relative to all other reactions, An asterisk indicates the Sog fragment resulting from cleavage at site 3, that is the most sensitive to high levels of Tsg (Shimmi and O'Connor, 2003) or as shown here to Srw. A) Control reactions demonstrating no cleavage or degradation of Sog in the absence of Tld. B) Basal cleavage level of Sog in the presence of Dpp and a predetermined aliquot of Tld S2 supernatant. Note that bands representing "full length Sog" and "site 1 cleavage Sog" are not well resolved. Also note that there is no cleavage at site 3 under these conditions. C) Addition of only a half dose of Tsg results in additional cleavage at site 2 compared to early time points (panel B) but no cleavage at site 3. D) Addition of Srw without Tsg results in modest cleavage of site 3 and additional cleavage at site 1 over time. E) Adding both Tsg and Srw results in robust cleavage at all three sites. F) Reducing Tld by half in the presence of both Tsg and Srw still results in robust cleavage at all three sites.

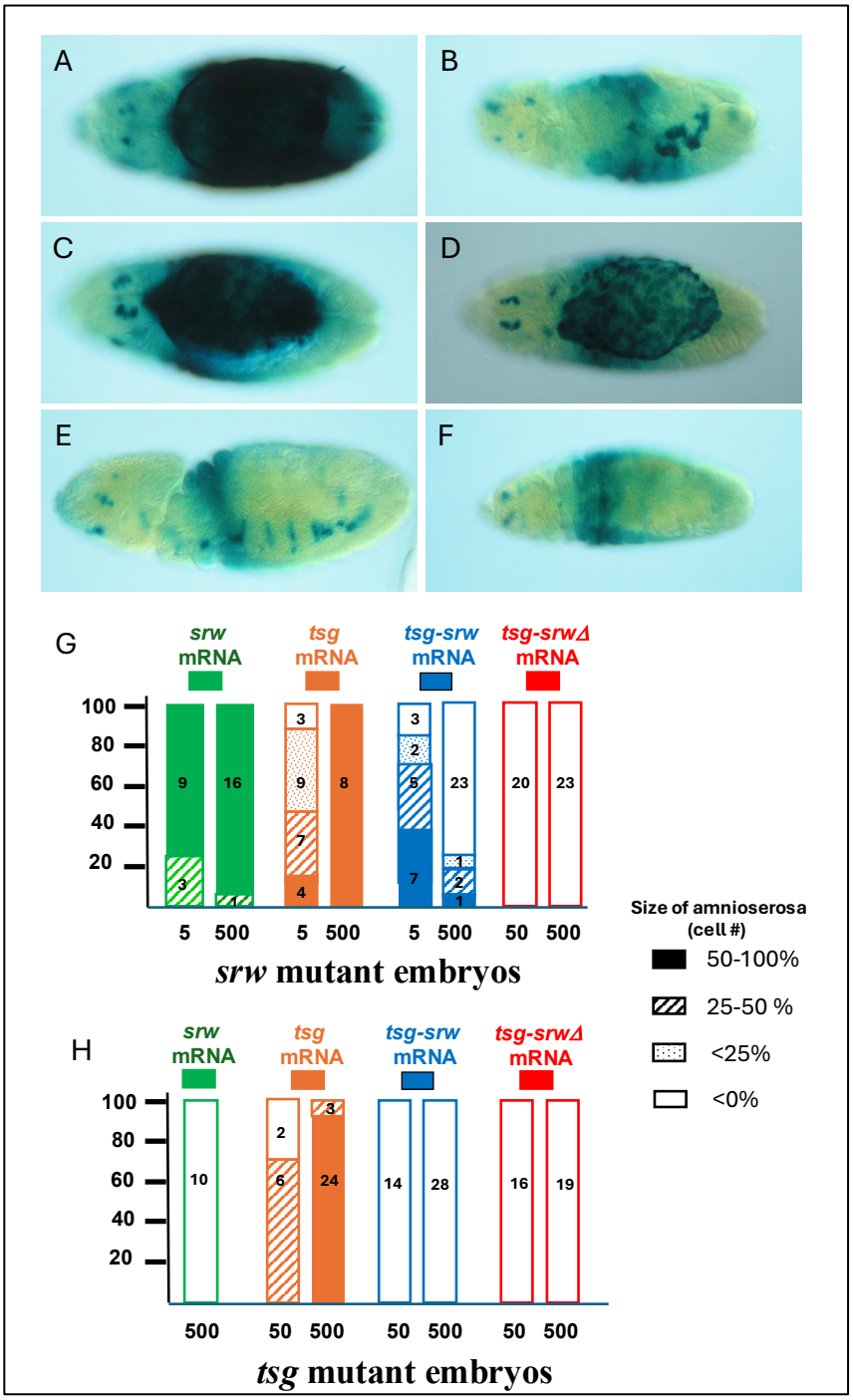

Fig. 5. Injection of *tsg* mRNA rescues *srw* mutants, but *srw* mRNA does not rescue *tsg* mutants. Embryos oriented with anterior to the left and dorsal to the top. A) srw^{B18} heterozygous embryo at stage 13 showing amnioserosa cells marked by Kr-LacZ expression. Kr-LacZ also drives expressions in a small number of anterior neurons. B) Ventralized srw^{B18} homozygous

mutant embryo at the same stage has a significant reduction in Kr-LacZ expression. C) Injection of 5 ng/µl *srw* mRNA into *srw* mutant embryos before stage 5 rescued the ventralized phenotype as shown by the amnioserosa at stage 13. D) Injection of 500 ng/µl *tsg* mRNA rescued the amnioserosa in the *srw* mutant. E) Injection of 500 ng/µl *srw* mRNA into a ventralized tsg^{YN97} hemizygous mutant embryo did not rescue. F) TsgΔSrw mRNA does not rescue the ventralized *tsg* phenotype. G) Quantification of rescue by indicated mRNAs injected into *srw* mutant embryos: X axis denotes concentration of mRNA in ng/ul, Y axis is the % positive AS (Amnioserosa) cells relative to wildtype embryos. The number of injected embryos binned to a particular rescue class is indicated in the shaded zones. H) Quantification of rescue by indicated mRNAs injected into *tsg* mutant embryos.

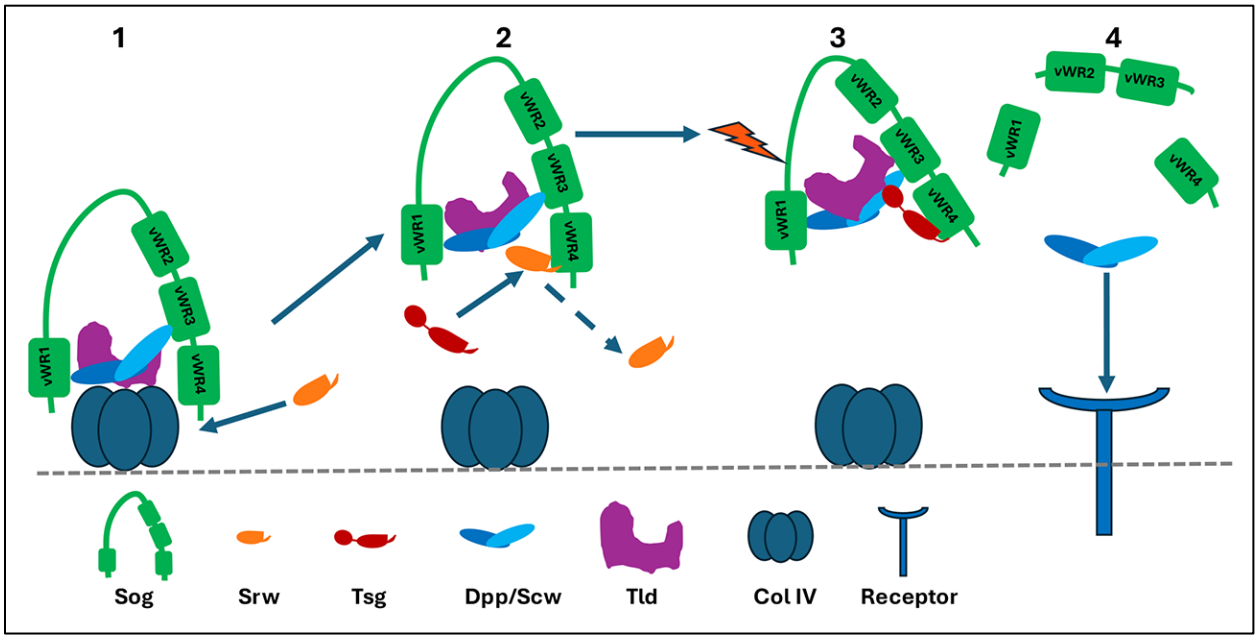

Fig. 6 Model for the role of Srw in embryonic Dpp gradient formation. 1) The Dpp-Scw heterodimer assembles on collagen IV together with Sog. 2) Srw displaces the Dpp-Scw-Sog complex from Collagen IV via an interaction between its α_2 helix and a VWF domain that binds to collagen IV. 3) Once displaced from collagen IV, Tsg assembles into the Dpp-Scw-Sog complex and is stabilized by both its α_2 interaction with a Sog VWF and its C-terminal tail with another VWF domain. This complex is now composed of Tsg-Sog-Dpp-Scw which can diffuse within the perivitelline space. The assembly with Tsg is speculated to stimulate a conformational change within the complex that enables Tld to access Sog cleavage sites. 4) Sog cleavage stimulates dissociation of the complex thereby freeing the Dpp-Scw heterodimer to either bind its receptor or to reassemble onto collagen IV. The relative probability of each option depends on the spatial position of the Dpp-Scw heterodimer along the D-V axis.

Supplemental figures (4) and tables (2)

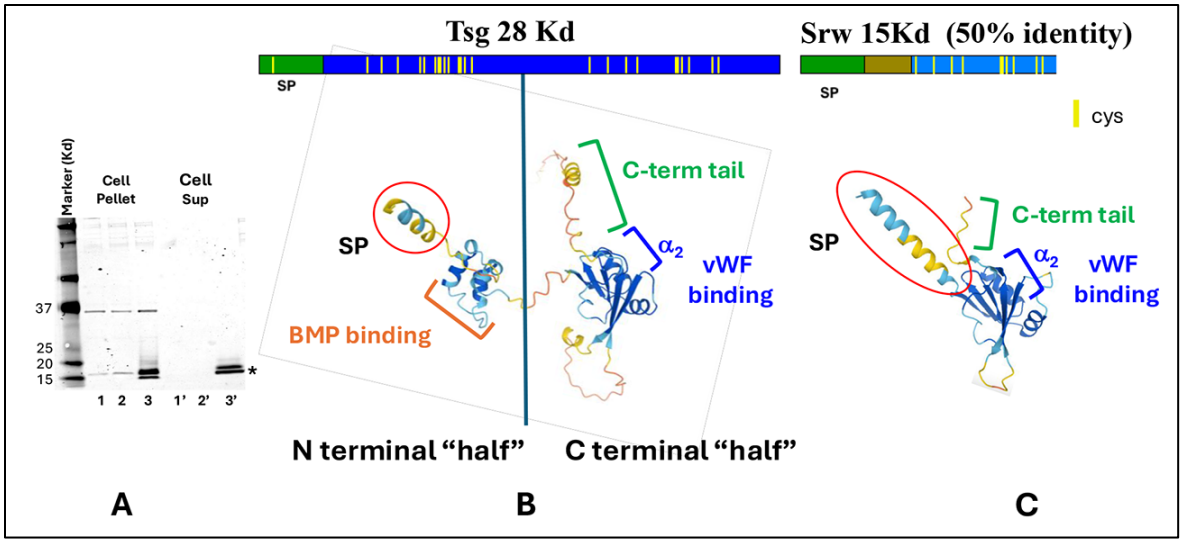

Fig. S1 Srw is a secreted and N-terminally truncated Tsg-like molecule. A) Western blot probed with anti-His antibody. Lanes 1-3 are the cell pellet fraction of ACPA empty vector, a Myo negative control, and Srw-His expression in S2 cells respectively. Lanes1'-3' are the same except showing the cell supernatant fractions. B) Top is a schematic representation of Tsg displaying the secretion signal peptide (SP) and cysteines in yellow. Bottom is an AlphaFold ribbon projection of Tsg with the N-terminal BMP-binding "half" on the left and the C-terminal Sog VWF interacting "half" on the right. The red circle denotes the SP. The α_2 helix that binds to a Sog VWF domain is indicated by a blue bracket. The C-terminal tail that has also been implicated in Sog VWF binding (Moore et al. 2024) is indicated by the green bracket. C) Top and bottom are a schematic representation and Alphafold ribbon projection of Srw with SP, cysteines, VWF binding domain and C-terminal tail shown. Srw has a similar arrangement of cysteine residues and is ~ 50% identical to the C-terminal domain of Tsg. AlphaFold projection is rotated to show a similar orientation of the most highly conserved regions (blue) between Tsg and Srw. Note that while Srw has similar positioning of the α_2 helix that binds to a Sog VWF, its C-terminal tail is much shorter, perhaps indicating that Srw cannot make two contacts with VWF domains as predicted for Tsg (Moore et al., 2024). This structural distinction may result in a more transient interaction between Srw and Sog than between Tsg and Sog.

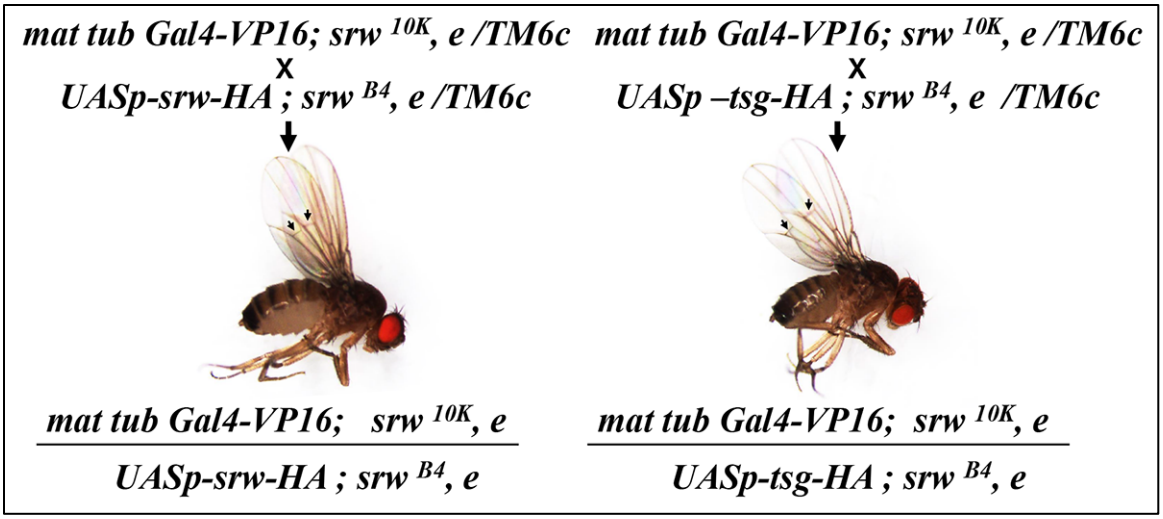

Fig. S2. Maternal expression of *tsg* rescues *srw* mutants fully with no patterning defects. Crosses were set up between males and females with the indicated genotypes. Rescue was determined by identifying ebony flies without a balancer chromosome. Examples of rescued flies are shown. Note that crossveins are present in the wings of rescued animals (small arrowheads) indicating that Srw is not required for patterning adult wings. More than 100 progeny were scored in both crosses. Rescue was ~120% of the expected Mendelian ratio, likely due to under-representation of flies carrying a balancer chromosome.

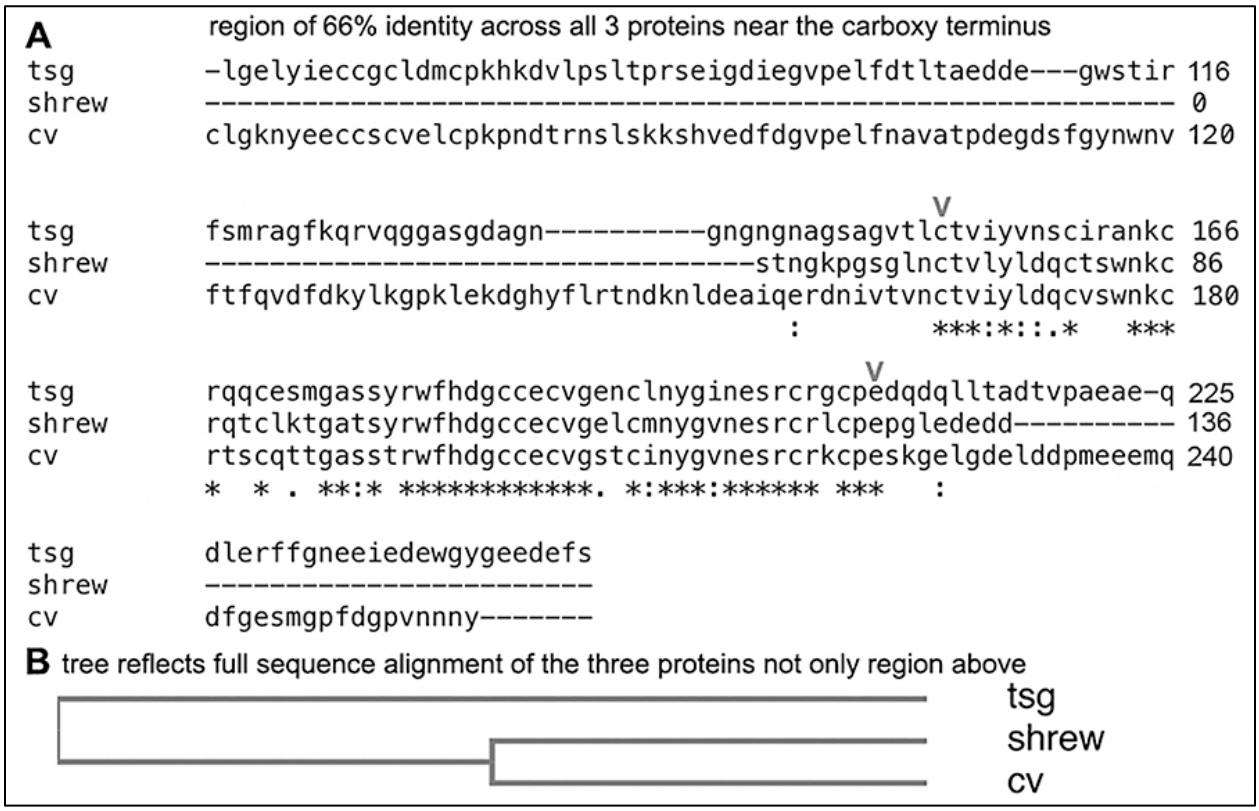

Fig. S3. ***D. melanogaster*** **Srw is 66% identical to both Tsg and Cv near the C-terminus but overall is most similar to Cv.** A) C-terminal half of Tsg, Cv and Srw aligned with identical amino acids marked by stars, similar amino acids marked by colons and amino acids similar only in a pair marked by a dot. Gaps computationally inserted to maximize similarity are shown by dashes. The beginning and end of a 57 amino acid region displaying 66% identity across the three sequences are marked with arrowheads. This region was utilized to search for Tsg family members in distant species. B) Neighbor joining tree of the Tsg family from a full-length alignment shows the clustering of Srw and Cv.

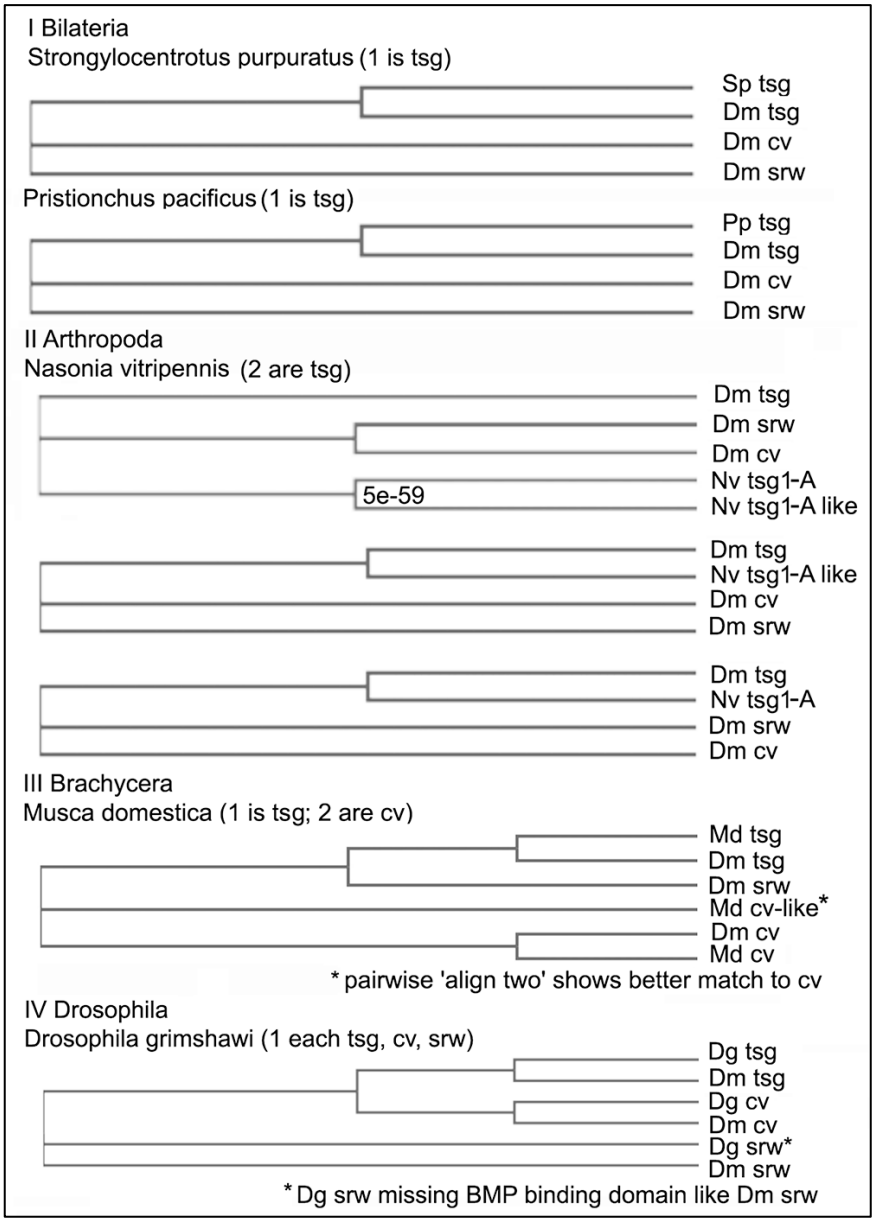

Fig. S4. Tsg family trees from exemplar species. One or two species from each subheading in Table 1 is shown with a tree of its Tsg family members. I) In Bilateria, the Deuterostome *Strongylocentrotus purpuratus* and the Protostome *Pristionchus pacificus* each have a single protein matching *D. melanogaster* Tsg. II) In Arthropods, *Nasonia vitripennis* has a recent duplication of Tsg as shown by the probability value of a BLASTp 'align two' analysis (5e-59). III) In Brachycera, *Musca domestica* has a recent duplication of Cv as shown by an 'align two' analysis. IV) In Drosophila, *D. grimshawi* has all three family members as shown by the absence of the amino terminal BMP binding domain in Srw and an 'align two' analysis.

Table S1. Exemplar species genome sequence details (as of 11/19/2023)

Species	Ref Seq[a]	Coverage	Assembly	Date
I. Metazoa to Priapulida				
Mnemiopsis leidyi (comb jellyfish)	Y	12X	Scaffold	09/19/2011
Nematostella vectensis (sea anemone)	Y	53X	Chromosome	03/23/2022
Meara stichopi (marine flatworm with no gut)	N			
Strongylocentrotus purpuratus (sea urchin)	Y	123X	Scaffold	09/06/2019
Mus musculus (house mouse)	Y	40X	Chromosome	06/24/2020
Octopus bimaculoides (California octopus)	Y	10X	Chromosome	10/06/2022
Caenorhabditis elegans (free living in soil)	Y	228X	Complete	02/07/2013
Pristionchus pacificus (symbiont of beetles)	Y	100X	Chromosome	11/02/2020
Trichinella pseudospiralis (human parasite)	Y	239X	Scaffold	11/24/2015
Priapulus caudatus (marine worm unsegmented)	Y	100X	Scaffold	11/19/2015
II. Arthropoda to Nematocera				
Limulus polyphemus (horseshoe crab)	Y	18X	Scaffold	01/03/2014
Tetranychus urticae (spider mite)	Y	8X	Scaffold	12/20/2011
Daphnia magna (water flea)	Y	243X	Chromosome	10/27/2021
Folsomia candida (springtail)	Y	58X	Scaffold	07/12/2017
Ladona fulva (dragonfly)	Y	131X	Scaffold	10/31/2017
Schistocerca gregaria (grasshopper)	Y	41X	Chromosome	06/24/2022
Aphis gossypii (cotton aphid)	Y	100X	Chromosome	09/30/2021
Tribolium castaneum (red flour beetle)	Y	7X	Chromosome	03/10/2016
Apis mellifera (european honey bee)	Y	192X	Chromosome	09/10/2018
Nasonia vitripennis (parasitoid wasps)	Y	142X	Chromosome	01/30/2020
Chrysoperla carnea (green lacewing)	Y	40X	Chromosome	04/15/2021
Bicyclus anynana (brown butterfly)	Y	20X	Chromosome	10/28/2022
Bombyx mori (silk moth)	Y	140X	Chromosome	10/13/2020
Anopheles darlingi (american mosquito)	Y	32X	Chromosome	06/04/2022
Phlebotomus papatasi (sandfly)	Y	14X	Chromosome	08/30/2022
III. Bracera to Drosophilini				
Musca domestica (house fly)	Y	135X	Scaffold	07/18/2023
Scaptodrosophila lebanonensis (vinegar fly)	Y	100X	Contig	05/29/2019
Zaprionus bogoriensis (white striped body)	Y	119X	Scaffold	12/17/2021
IV. Drosophila genus				
Drosophila griimshawi	Y	93X	Contig	04/28/2021
Drosophila hydei	Y	120X	Contig	05/29/2019
Drosophila melanogaster	Y	30X	Chromosome	08/01/2014

a. NCBI Reference Sequence Assembly

Table S2. GenBank Protein Accession numbers

Species	Accession	Description (results this study)
I. Metazoa to Priapulida		
Meara stichopi	AVK72344	Tsg
Strongylocentrotus purpuratus	XP_794111	Tsg homolog 1-A
Mus musculus	NP_075540	Tsg homolog 1 precursor
Octopus bimaculoides	XP_014790371	Tsg homolog 1-A
Pristionchus pacificus	KAF8367969	Hypothetical: PRIPAC 85798 (Tsg)
Trichinella pseudospirali	KRY68079	Tsg
Priapulus caudatus	XP_014672210	Predicted: Tsg homolog 1-A-like
II. Arthropoda to Nematocera		
Limulus polyphemus	XP_013785056	Tsg homolog 1-like
	XP_013777713	Tsg-like
Tetranychus urticae	XP_015789659	Tsg
Daphnia magna	XP_032785398	Tsg homolog 1-A
Folsomia candida	XP_021966353	Tsg
Ladona fulva	KAG8233409	Hypothetical: J437 LFUL013402 (Tsg)
Schistocerca gregaria	XP_049827500.	Tsg-like
Aphis gossypii	XP_027844935	Tsg
Tribolium castaneum	XP_001812776	Predicted: Tsg
Apis mellifera	XP_006559045	Tsg homolog 1-A
Nasonia vitripennis	XP_001600362	Tsg homolog 1-A
	XP_016837111	Tsg homolog 1-A-like
Chrysoperla carnea	XP_044732655	Tsg-like
Bicyclus anynana	XP_052743694	Tsg
Bombyx mori	XP_004933428	Tsg
Anopheles darlingi	XP_049542551	Tsg-like
	XP_049538285	Tsg-like isoform X2
Phlebotomus papatasi	XP_055712455	Tsg-like
III. Brachycera to Drosophilini		
Musca domestica	XP_005177880	Tsg
	XP_005186377	Tsg (Cv)
	XP_005177270	Tsg (Cv)
Scaptodrosophila lebanonensis	XP_030379739	Tsg
	XP_030378124	Tsg (Cv)
Zaprionus bogoriensis	KAH8416613	Hypothetical: KR222_011407 (Tsg)
	KAH8396273	Hypothetical: KR222_007228 (Cv)
IV. Drosophila genus		
Drosophila griimshawi	XP_001991879	Tsg
	XP_001991474	Tsg (Cv)
	XP_001983521	Tsg (Srw)
Drosophila hydei	XP_023160278	Tsg
	XP_023161952	Tsg (Cv)
	XP_023164684	Tsg (Srw)
Drosophila melanogaster	>NP_511135	Tsg
	NP_536786.1	Cv
	NP_647886.2	Srw

Literature Cited

Abramson J, Adler J, Dunger J, Evans R, Green T, Pritzel A, Ronneberger O, Willmore L, Ballard AJ, Bambrick J. et al. (2024) Accurate structure prediction of biomolecular interactions with AlphaFold3. *Nature* **630**, 493-500.

Akiyama, T., Raftery, L. A. and Wharton, K. A. (2024). Bone morphogenetic protein signaling: the pathway and its regulation. *Genetics* **226**.

Anderson D, T. (1972). *The development of holometabolous insects*. New York: Academic Press.

Angelichio, M. L., Beck, J. A., Johansen, H. and Ivey-Hoyle, M. (1991). Comparison of several promoters and polyadenylation signals for use in heterologous gene expression in cultured Drosophila cells. *Nucleic Acids Res* **19**, 5037-5043.

Ashe, H. L., Mannervik, M. and Levine, M. (2000). Dpp signaling thresholds in the dorsal ectoderm of the Drosophila embryo. *Development* **127**, 3305-3312.

Benton, M. A., Akam, M. and Pavlopoulos, A. (2013). Cell and tissue dynamics during Tribolium embryogenesis revealed by versatile fluorescence labeling approaches. *Development* **140**, 3210-3220.

Bonds, M., Sands, J., Poulson, W., Harvey, C. and Von Ohlen, T. (2007). Genetic screen for regulators of ind expression identifies shrew as encoding a novel twisted gastrulation-like protein involved in Dpp signaling. *Dev Dyn* **236**, 3524-3531.

Brown, N. H. and Kafatos, F. C. (1988). Functional cDNA libraries from Drosophila embryos. *J Mol Biol* **203**, 425-437.

Calderon, D., Blecher-Gonen, R., Huang, X., Secchia, S., Kentro, J., Daza, R. M., Martin, B., Dulja, A., Schaub, C., Trapnell, C., et al. (2022). The continuum of. *Science* **377**, eabn5800.

Chen, J., Honeyager, S. M., Schleede, J., Avanesov, A., Laughon, A. and Blair, S. S. (2012). Crossveinless d is a vitellogenin-like lipoprotein that binds BMPs and HSPGs, and is required for normal BMP signaling in the Drosophila wing. *Development* **139**, 2170-2176.

Cheng, S., Jacobs, C. Mogollón Pérez, E. Chen, D., van de Sanden, J. T., Bretscher, K. M., Verweij, F., Bosman, J. S., Hackmann, A., Merks, R. M. H., et al. (2024). A life-history allele of large effect shortens developmental time in a wild insect population. *Nat Ecol Evol* **8**, 70-82.

Chong, J., Amourda, C. and Saunders, T. E. (2018). Temporal development of. *J R Soc Interface* **15**.

Church, S. H., Donoughe, S., de Medeiros, B. A. S. and Extavour, C. G. (2019a). A dataset of egg size and shape from more than 6,700 insect species. *Sci Data* **6**, 104.

---- (2019b). Insect egg size and shape evolve with ecology but not developmental rate. *Nature* **571**, 58-62.

De Robertis, E. M. and Tejeda-Muñoz, N. (2022). Evo-Devo of Urbilateria and its larval forms. *Dev Biol* **487**, 10-20.

de Vienne, D. M. (2016). Lifemap: exploring the entire tree of life. *PLoS Biol* **14**, e2001624.

Dearden, P. K. and Akam, M. (2001). Early embryo patterning in the grasshopper, Schistocerca gregaria: wingless, decapentaplegic and caudal expression. *Development* **128**, 3435-3444.

Disney, R. H. (2008). Natural history of the scuttle fly, Megaselia scalaris. *Annu Rev Entomol* **53**, 39-60.

Eldar, A., Dorfman, R., Weiss, D., Ashe, H., Shilo, B. Z. and Barkai, N. (2002). Robustness of the BMP morphogen gradient in Drosophila embryonic patterning. *Nature* **419**, 304-308.

Fen, X., Ke, L. and Zeng, J. (2019). Histomorphological study on embryogenesis of the honeybee Apis cerana. *J. Asia Pac. Entom.* **22**, 860-867.

Ferguson, E. L. and Anderson, K. V. (1992a). Decapentaplegic acts as a morphogen to organize dorsal-ventral pattern in the Drosophila embryo. *Cell* **71**, 451-461.

---- (1992b). Localized enhancement and repression of the activity of the TGF-beta family member, decapentaplegic, is necessary for dorsal-ventral pattern formation in the Drosophila embryo. *Development* **114**, 583-597.

Francois, V., Solloway, M., O'Neill, J. W., Emery, J. and Bier, E. (1994). Dorsal-ventral patterning of the Drosophila embryo depends on a putative negative growth factor encoded by the short gastrulation gene. *Genes Dev* **8**, 2602-2616.

Gavin-Smyth, J., Wang, Y. C., Butler, I. and Ferguson, E. L. (2013). A genetic network conferring canalization to a bistable patterning system in Drosophila. *Curr Biol* **23**, 2296-2302.

Goltsev, Y., Rezende, G. L., Vranizan, K., Lanzaro, G., Valle, D. and Levine, M. (2009). Developmental and evolutionary basis for drought tolerance of the Anopheles gambiae embryo. *Dev Biol* **330**, 462-470.

Haerry, T. E. and O'Connor, M. B. (2002). Isolation of Drosophila activin and follistatin cDNAs using novel MACH amplification protocols. *Gene* **291**, 85-93.

Hermann, S. L., Blackledge, C., Haan, N. L., Myers, A. T. and Landis, D. A. (2019). Predators of monarch butterfly eggs and neonate larvae are more diverse than previously recognised. *Sci Rep* **9**, 14304.

Jumper J, Evans R, Pritzel A, Green T, Figurnov M, Ronneberger O, Tunyasuvunakool K, Bates R, Žídek A, Potapenko A. et al. (2021) Highly accurate protein structure prediction with AlphaFold. Nature. **596** 583-589.

Jürgens, G., Wieschaus, E., Nüsslein-Volhard, C. and Kluding, H. (1984). Mutations affecting the pattern of the larval cuticle inDrosophila melanogaster : II. Zygotic loci on the third chromosome. *Wilehm Roux Arch Dev Biol* **193**, 283-295.

Katagiri, T. and Watabe, T. (2016). Bone Morphogenetic Proteins. *Cold Spring Harb Perspect Biol* **8**.

Koch, R., Ledermann, R., Urwyler, O., Heller, M. and Suter, B. (2009). Systematic functional analysis of Bicaudal-D serine phosphorylation and intragenic suppression of a female sterile allele of BicD. *PLoS One* **4**, e4552.

Kumar, S., Suleski, M., Craig, J. M., Kasprowicz, A. E., Sanderford, M., Li, M., Stecher, G. and Hedges, S. B. (2022). TimeTree 5: An Expanded Resource for Species Divergence Times. *Mol Biol Evol* **39**.

Kwan, C. W., Gavin-Smyth, J., Ferguson, E. L. and Schmidt-Ott, U. (2016). Functional evolution of a morphogenetic gradient. *Elife* **5**.

Larraín, J., Oelgeschläger, M., Ketpura, N. I., Reversade, B., Zakin, L. and De Robertis, E. M. (2001). Proteolytic cleavage of Chordin as a switch for the dual activities of Twisted gastrulation in BMP signaling. *Development* **128**, 4439-4447.

Li, F., Rane, R. V., Luria, V., Xiong, Z., Chen, J., Li, Z., Catullo, R. A., Griffin, P. C., Schiffer, M., Pearce, S., et al. (2022). Phylogenomic analyses of the genus Drosophila reveals genomic signals of climate adaptation. *Mol Ecol Resour* **22**, 1559-1581.

Madamanchi, A., Mullins, M. C. and Umulis, D. M. (2021). Diversity and robustness of bone morphogenetic protein pattern formation. *Development* **148**.

Madeira F, Madhusoodanan N, Lee J, Eusebi A, Niewielska A, Tivey ARN, Meacham S, Lopez R, Butcher S. (2024) Using EMBL-EBI Services via Web Interface and Programmatically via Web Services. *Curr Protoc.* **4**, e1065.

Malinauskas, T., Moore, G., Rudolf, A. F., Eggington, H., Belnoue-Davis, H. L., El Omari, K., Griffiths, S. C., Woolley, R. E., Duman, R., Wagner, A., et al. (2024). Molecular mechanism of BMP signal control by Twisted gastrulation. *Nat Commun* **15**, 4976.

Markow, T. A. (2015). The secret lives of Drosophila flies. *Elife* **4**.

Marques, G., Musacchio, M., Shimell, M. J., Wunnenberg-Stapleton, K., Cho, K. W. and O'Connor, M. B. (1997). Production of a DPP activity gradient in the early Drosophila embryo through the opposing actions of the SOG and TLD proteins. *Cell* **91**, 417-426.

Mason, E. D., Konrad, K. D., Webb, C. D. and Marsh, J. L. (1994). Dorsal midline fate in Drosophila embryos requires twisted gastrulation, a gene encoding a secreted protein related to human connective tissue growth factor. *Genes Dev* **8**, 1489-1501.

Matsuda, S., Harmansa, S. and Affolter, M. (2016). BMP morphogen gradients in flies. *Cytokine Growth Factor Rev* **27**, 119-127.

Mirdita M, Schütze K, Moriwaki Y, Heo L, Ovchinnikov S, Steinegger M. (2022). ColabFold: making protein folding accessible to all. *Nat Methods* **19**, 679-682.

Mitchison, T. J. and Sedat, J. (1983). Localization of antigenic determinants in whole Drosophila embryos. *Dev Biol* **99**, 261-264.

Mizutani, C. M., Nie, Q., Wan, F. Y., Zhang, Y. T., Vilmos, P., Sousa-Neves, R., Bier, E., Marsh, J. L. and Lander, A. D. (2005). Formation of the BMP activity gradient in the Drosophila embryo. *Dev Cell* **8**, 915-924.

Moali, C., Font, B., Ruggiero, F., Eichenberger, D., Rousselle, P., François, V., Oldberg, A., Bruckner-Tuderman, L. and Hulmes, D. J. (2005). Substrate-specific modulation of a multisubstrate proteinase. C-terminal processing of fibrillar procollagens is the only BMP-1-dependent activity to be enhanced by PCPE-1. *J Biol Chem* **280**, 24188-24194.

Moore G, Revici R, Beadle L, Birchenough H,Baldock C, Ashe H (2024) An avidity-driven mechanism of extracellular BMP regulation by Twisted gastrulation. bioRxiv (preprint) doi.org/10.1101/2024.07.08.602551

Mörsdorf, D., Knabl, P. and Genikhovich, G. (2024). Highly conserved and extremely evolvable: BMP signalling in secondary axis patterning of Cnidaria and Bilateria. *Dev Genes Evol* **234**, 1-19.

Nakao, H. (2021). Early embryonic development of Bombyx. *Dev Genes Evol* **231**, 95-107.

Nichols, S. A., Dirks, W., Pearse, J. S. and King, N. (2006). Early evolution of animal cell signaling and adhesion genes. *Proc Natl Acad Sci U S A* **103**, 12451-12456.

Nunes da Fonseca, R., van der Zee, M. and Roth, S. (2010). Evolution of extracellular Dpp modulators in insects: The roles of tolloid and twisted-gastrulation in dorsoventral patterning of the Tribolium embryo. *Dev Biol* **345**, 80-93.

O'Connor, M. B., Umulis, D., Othmer, H. G. and Blair, S. S. (2006). Shaping BMP morphogen gradients in the Drosophila embryo and pupal wing. *Development* **133**, 183-193.

Oelgeschläger, M., Larraín, J., Geissert, D. and De Robertis, E. M. (2000). The evolutionarily conserved BMP-binding protein Twisted gastrulation promotes BMP signalling. *Nature* **405**, 757-763.

Parvy, J. P., Blais, C., Bernard, F., Warren, J. T., Petryk, A., Gilbert, L. I., O'Connor, M. B. and Dauphin-Villemant, C. (2005). A role for betaFTZ-F1 in regulating ecdysteroid titers during post-embryonic development in Drosophila melanogaster. *Dev Biol* **282**, 84-94.

Pfeiffer D, Shrader M, Wahls J, Willbrand B, Sandum I, et al. (2019) African fig fly (Diptera: Drosophilidae): biology, expansion of geographic range, and its potential status as a soft fruit pest. *J Integr Pest Manag* **10,** 1–8.

Rafiqi, A. M., Park, C. H., Kwan, C. W., Lemke, S. and Schmidt-Ott, U. (2012). BMP-dependent serosa and amnion specification in the scuttle fly Megaselia abdita. *Development* **139**, 3373-3382.

Raftery, L. A. and Sutherland, D. J. (2003). Gradients and thresholds: BMP response gradients unveiled in Drosophila embryos. *Trends Genet* **19**, 701-708.

Rørth, P. (1998). Gal4 in the Drosophila female germline. *Mech Dev* **78**, 113-118.

Sachs, L., Chen, Y. T., Drechsler, A., Lynch, J. A., Panfilio, K. A., Lässig, M., Berg, J. and Roth, S. (2015). Dynamic BMP signaling polarized by Toll patterns the dorsoventral axis in a hemimetabolous insect. *Elife* **4**, e05502.

Sawala, A., Scarcia, M., Sutcliffe, C., Wilcockson, S. G. and Ashe, H. L. (2015). Peak BMP Responses in the Drosophila Embryo Are Dependent on the Activation of Integrin Signaling. *Cell Rep* **13**, 1519-1520.

Sawala, A., Sutcliffe, C. and Ashe, H. L. (2012). Multistep molecular mechanism for bone morphogenetic protein extracellular transport in the Drosophila embryo. *Proc Natl Acad Sci USA* **109**, 11222-11227.

Schmidt-Ott, U. and Kwan, C. W. (2022). How two extraembryonic epithelia became one: serosa and amnion features and functions of. *Philos Trans R Soc Lond B Biol Sci* **377**, 20210265.

Scott, I. C., Blitz, I. L., Pappano, W. N., Maas, S. A., Cho, K. W. and Greenspan, D. S. (2001). Homologues of Twisted gastrulation are extracellular cofactors in antagonism of BMP signalling. *Nature* **410**, 475-478.

Serpe, M., Ralston, A., Blair, S. S. and O'Connor, M. B. (2005). Matching catalytic activity to developmental function: tolloid-related processes Sog in order to help specify the posterior crossvein in the Drosophila wing. *Development* **132**, 2645-2656.

Serpe, M., Umulis, D., Ralston, A., Chen, J., Olson, D. J., Avanesov, A., Othmer, H., O'Connor, M. B. and Blair, S. S. (2008). The BMP-binding protein Crossveinless 2 is a short-range, concentration-dependent, biphasic modulator of BMP signaling in Drosophila. *Dev Cell* **14**, 940-953.

Shimell, M. J., Ferguson, E. L., Childs, S. R. and O'Connor, M. B. (1991). The Drosophila dorsal-ventral patterning gene tolloid is related to human bone morphogenetic protein 1. *Cell* **67**, 469-481.

Shimmi, O. and O'Connor, M. B. (2003). Physical properties of Tld, Sog, Tsg and Dpp protein interactions are predicted to help create a sharp boundary in Bmp signals during dorsoventral patterning of the Drosophila embryo. *Development* **130**, 4673-4682.

Shimmi, O., Ralston, A., Blair, S. S. and O'Connor, M. B. (2005a). The crossveinless gene encodes a new member of the Twisted gastrulation family of BMP-binding proteins which, with Short gastrulation, promotes BMP signaling in the crossveins of the Drosophila wing. *Dev Biol* **282**, 70-83.

Shimmi, O., Umulis, D., Othmer, H. and O'Connor, M. B. (2005b). Facilitated transport of a Dpp-Scw heterodimer by Sog/Tsg leads to robust patterning of the Drosophila blastoderm embryo. *Cell* **120**, 873-886.

Simon, S., Sagasser, S., Saccenti, E., Brugler, M. R., Schranz, M. E., Hadrys, H., Amato, G. and DeSalle, R. (2017). Comparative transcriptomics reveal developmental turning points during embryogenesis of a hemimetabolous insect, damselfly Ischnura elegans. *Sci Rep* **7**, 13547.

Souza, A., Souza, B., Bezerra, C. and Amaral, B. (2016). Facilitated harvesting of eggs from lab reared C*hrysoperla externa* (Neuroptera: Chrysopidae).*Revista Colomb. Entom.* **42**, 133-136.

St Johnston, R. D. and Gelbart, W. M. (1987). Decapentaplegic transcripts are localized along the dorsal-ventral axis of the Drosophila embryo. *EMBO J* **6**, 2785-2791.

Suga, H., Ono, K. and Miyata, T. (1999). Multiple TGF-beta receptor related genes in sponge and ancient gene duplications before the parazoan-eumetazoan split. *FEBS Lett* **453**, 346-350.

Sutherland, D. J., Li, M., Liu, X. Q., Stefancsik, R. and Raftery, L. A. (2003). Stepwise formation of a SMAD activity gradient during dorsal-ventral patterning of the Drosophila embryo. *Development* **130**, 5705-5716.

Throckmorton, L. (1975). *The phylogeny, ecology and geography of Drosophila*. New York: Plenum.

Tyers, M., Tokiwa, G., Nash, R. and Futcher, B. (1992). The Cln3-Cdc28 kinase complex of S. cerevisiae is regulated by proteolysis and phosphorylation. *EMBO J* **11**, 1773-1784.

Umulis, D., O'Connor, M. B. and Blair, S. S. (2009). The extracellular regulation of bone morphogenetic protein signaling. *Development* **136**, 3715-3728.

Umulis, D. M., Serpe, M., O'Connor, M. B. and Othmer, H. G. (2006). Robust, patterning of the dorsal surface of the Drosophila embryo. *Proc Natl Acad Sci U S A* **103**, 11613-11618.

Umulis, D. M., Shimmi, O., O'Connor, M. B. and Othmer, H. G. (2010). Organism-scale modeling of early Drosophila patterning via bone morphogenetic proteins. *Dev Cell* **18**, 260-274.

Upadhyay, A., Moss-Taylor, L., Kim, M. J., Ghosh, A. C. and O'Connor, M. B. (2017). TGF-β Family Signaling in. *Cold Spring Harb Perspect Biol* **9**.

Varadi M, Bertoni D, Magana P, Paramval U, Pidruchna I, Radhakrishnan M, Tsenkov M, Nair S, Mirdita M, Yeo J. et al. (2024) AlphaFold Protein Structure Database 2024: providing structure coverage for over 214 million protein sequences. *Nucleic Acids Res.* **52,** D368-D375.

Wang, X., Harris, R. E., Bayston, L. J. and Ashe, H. L. (2008). Type IV collagens regulate BMP signalling in Drosophila. *Nature* **455**, 72-77.

Wang, Y. C. and Ferguson, E. L. (2005). Spatial bistability of Dpp-receptor interactions during Drosophila dorsal-ventral patterning. *Nature* **434**, 229-234.

Wharton, K. A., Ray, R. P. and Gelbart, W. M. (1993). An activity gradient of decapentaplegic is necessary for the specification of dorsal pattern elements in the Drosophila embryo. *Development* **117**, 807-822.

Winstanley, J., Sawala, A., Baldock, C. and Ashe, H. L. (2015). Synthetic enzyme-substrate tethering obviates the Tolloid-ECM interaction in Drosophila BMP gradient formation. *Elife* **4**.

Wisotzkey, R. G. and Newfeld, S. J. (2020). TGF-β Prodomain Alignments Reveal Unexpected Cysteine Conservation Consistent with Phylogenetic Predictions of Cross-Subfamily Heterodimerization. *Genetics* **214**, 447-465.

Wotton, K. R. (2014). Heterochronic shifts in germband movements contribute to the rapid embryonic development of the coffin fly Megaselia scalaris. *Arthropod Struct Dev* **43**, 589-594.

Xie, J. and Fisher, S. (2005). Twisted gastrulation enhances BMP signaling through chordin dependent and independent mechanisms. *Development* **132**, 383-391.

Zalucki, M. P., Clarke, A. R. and Malcolm, S. B. (2002). Ecology and behavior of first instar larval Lepidoptera. *Annu Rev Entomol* **47**, 361-393.